Simulation of Proton in Silicon using GEANT4 for Beam Lifetime 3 Experiment

by

Jabia Moazam

A thesis submitted to
The Faculty of Graduate Studies of The University of Manitoba
in partial fulfillment of the requirements of the degree of

Master of Science

Department of Physics and Astronomy
The University of Manitoba
Winnipeg, Manitoba, Canada

January 2024

Thesis Advisor
Dr. Wouter Deconinck

Author
Jabia Moazam

Abstract

The Beam Lifetime 3 (BL3) experiment at the National Institute of Standards and Technology, USA, aims to improve the precision of neutron lifetime measurements and will hopefully resolve the inconsistency between beam and bottle measurements of the neutron lifetime by enhancing the precision of this beam measurement. In the BL3 experiment, where protons from neutron decay are detected in a silicon detector, a GEANT4-based simulation was used to model, develop, and optimize the experimental setup. The physics list, used to simulate particle transportation and interactions, was derived from one of the advanced examples of GEANT4 and extended with a screened nuclear recoil model appropriate for low-energy proton-nucleus scattering of protons in silicon. This approach will allow the many applications of the SRIM (Stopping and Range of Ions in Matter) software for modelling these interactions to be expanded into the much more general GEANT4 framework where nuclear and other effects can be included. By using the example in TestEm7/StandardNR, G4BL3/SNR, and the physics list in GEANT4, the energy deposition and backscattering/ transmission of 35 keV protons on a silicon detector are studied. Comparing the outcomes with SRIM and confirming the energy accumulation in GEANT4's numerous processes and its effects on the ratio of various components are being analyzed.

Table of Contents

List of Figures

List of Tables

Acknowledgments

First, I would like to thank my professors, staff and fellow students who supported me in pursuing higher education in physics. I wish to express my gratitude to Dr. Wouter Deconinck, my current supervisor, for leading me through most of my graduate research career. His persistent dedication to seeing me succeed academically has been a consistent source of inspiration. I sincerely appreciate the time and work Dr. Wouter has put into helping me with my thesis and academic progress.

I would like to express my sincere gratitude to my thesis committee members, Dr. Gerald Gwinner and Dr. Michael Gericke. Their invaluable guidance, feedback, and support have been instrumental in the completion of this work. I am grateful for their time, dedication, and commitment to my academic and professional development. In addition, I want to thank Susan Beshta and Maiko Langelaar at the Department of Physics and Astronomy for their excellent administrative and technical support.

I would like to express the highest degree of love and thankfulness to my parents, sisters, and brother Malik Abdullah Shaukat for always having my back no matter what happens. Especially to my parents, whose sacrifices and devotion, despite the midst of challenges and struggle, truly brought me into the person I am. Mom and Dad, you have always been my biggest supporters. From the earliest days of my academic journey, you taught me the importance of education, and you never wavered in your belief that I could achieve anything I set my mind to. Your unwavering support, both financially and emotionally, has made all the difference.

I wanted to take a moment to thank my spouse Moazam Mahmood for his constant support while I was pursuing my graduate degree. I could not have finished my thesis without your support, kindness, and patience. Your belief in me and constant support kept me going during the toughest of times. I could not have done this without you. Also, thanks to my Kids, Moeez, Maaz, Mahroosh and Momin who have been my inspiration throughout this journey. Their boundless energy and enthusiasm for life never cease to amaze me. Their understanding of why

Mom had to spend so many hours at her desk, and their patience with me when I had to miss some of their activities, made all the difference.

I am grateful to have such an amazing family, and I hope this thesis is a testament to the sacrifices we have all made along the way. Thank you for being my cheerleaders, my sounding boards, and my constant source of love and support. I love you all more than words can say.

Dedication

To my late father “Malik Shaukat Ali” for his endless love, and encouragement which I will always remember as my source of inspiration, support, and guidance, he always taught me to be unique and determined and to believe in myself.

Chapter 1

Introduction

1.1 Beam Lifetime 3 Experiment

The Beam Lifetime 3 (BL3) experiment at the National Institute of Standards and Technology in the United States is focused on improving the accuracy of neutron lifetime data. This might put an end to the long-standing contradiction between the two approaches to measuring the neutron lifetime: the beam and the bottle method. The two techniques' estimates of neutron lifetime vary by about 10 seconds. The continued discrepancy may imply new physical processes, such as neutron oscillations and low-energy physics in dark sectors.

In the BL3 experiment the decaying protons of the collimated beam of cold neutrons are trapped by the electrostatic and electromagnetic fields of a quasi-penning trap. To determine the weak decay lifetimes, we accumulate trapped protons from the beam of neutrons that decay as they pass through the trap, then gradually decrease the electric field on one side of the trap allowing the protons to reach a silicon detector. The BL3 project's infrastructure is funded by the US National Science Foundation. The Canadian contribution's immediate focus is on simulating decaying protons in the trap as well as testing a prototype proton detector at a 30 keV mass spectrometer.

The development of a Beam Lifetime 3 experiment is ongoing. New, larger magnets and traps are being used compared to the Beam Lifetime 2 experiment to manage larger neutron beams and improve the proton counting rate, leading to better statistical precision and the ability to conduct systematic studies. These protons follow a bend in the magnetic field to a silicon detector when the trap is periodically opened, where the larger neutron beam is projected on a larger silicon detector than before. The neutron density is measured by passing the same neutron beam through a thin-foil neutron counter, another improvement over the previous generation of beam measurements.

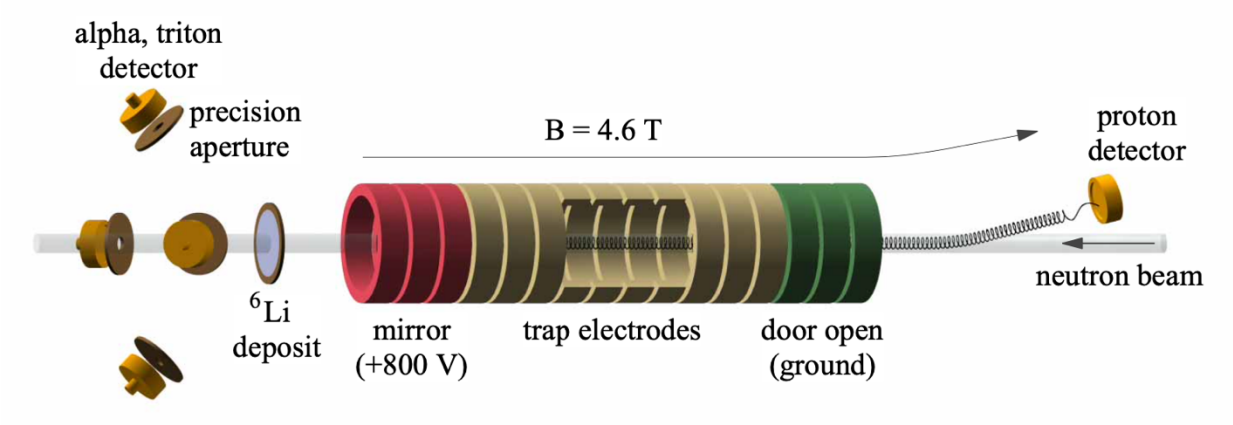

Figure 1. 1 An image of a lifetime measurement method using a cold neutron beam at NIST [1].

The Beam Lifetime 3 (BL3) experiment at the National Institute of Standards and Technology (NIST) calculates the neutron lifetime by detecting neutron decaying, in contrast to the UCNtau experiment [1]. The neutron lifetime might be determined by comparing the rate of beta-decay protons gathered in the trap with the rate of beam neutrons going through the Penning trap. A Penning trap is a device used in physics to trap charged particles (usually ions) using a combination of magnetic and electric fields.

The physical conversion of a neutron into a proton or vice versa inside an atomic nucleus to create the nucleus of a neighbouring element in the periodic table is known as nuclear beta decay. The charged-current weak interaction, which permits up and down quarks to switch identities, is fundamental to beta decay [1].

1.2 History of Neutrons and Role in Physics

By 1920, scientists realized that most of the atom's mass was made up of the protons and neutrons in its core nucleus. James Chadwick said in May 1932 that atomic nuclei also include a new type of neutral particles called neutrons. Around 1930, numerous researchers began bombarding beryllium with alpha particles from a polonium source to study the radiation emitted by the metal, including German physicist Walter Bothe and his student Herbert Becker. Some scientists claimed that the especially penetrating radiation from beryllium was composed of

extremely energetic photons. After seeing several strange properties of this radiation, Chadwick started to wonder if it may be composed of neutral particles, as Rutherford had proposed.

In February 1932, Chadwick published a paper titled "Possibility of the Existence of Neutrons" after just two weeks of testing [2]. According to the paper, neutron evidence should be employed rather than gamma-ray photons to solve the puzzle of Speake radiation. A few months later, in May 1932, Chadwick delivered a more detailed study titled "The Presence of the Neutron." His experimental setup is shown schematically in the image below [2]. A paraffin layer is positioned in front of the cloud chamber, which is filled with high-energy radiation coming from the polonium-beryllium (Po-Be) source on the left side. Radiation is scattered by a proton in the paraffin and the proton that recoils is photographed in the cloud chamber to the right.

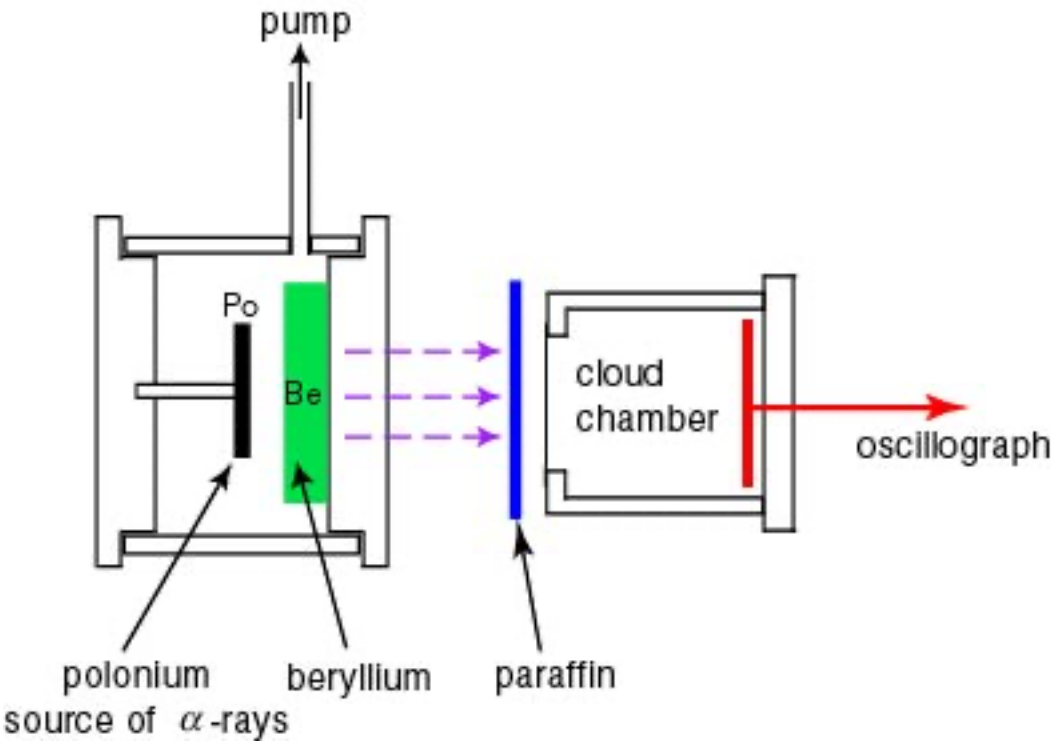

Figure 1. 2 Experimental Apparatus of Chadwick [2].

Chadwick subjected sources of helium and nitrogen (Po-Be) to radiation in addition to protons (paraffin). Chadwick concluded that it is not possible to interpret the mysterious radiation

originating from (Po-Be) sources as gamma radiation after analyzing the findings of this research. He ultimately concluded that everything could be reliably explained if the mysterious radiation was an electrically neutral particle with about the same mass as a proton. This proved the existence of the theoretical "neutral proton" that Rutherford predicted. This material was referred to by Chadwick as a "neutron" (1932).

After this discovery, many scientists worldwide focused on the characteristics and interactions of particles. Apart from simple hydrogen, all atoms have neutrons in their nuclei. Because they have no electrical charge and are neutral. When nuclear scientists first started researching neutron lifetimes, they discovered the significance of the neutron in physics. The neutron is one of the simplest radioactive particles. The neutron lifetime is one of the most important fundamental constants for cosmology and the weak interaction theory.

Nuclear fission happens when neutrons strike different elements. A heavy element's nucleus splitting into two roughly equal tiny fragments causes this type of nuclear reaction to take place. It is also feasible to manufacture significant quantities of valuable radioactive isotopes for a variety of uses due to the neutron absorption by nuclei exposed to the high neutron intensities present in nuclear reactors. The data about the atomic nucleus and the pressure holding it together are found in the nuclear reactions caused by neutrons. Elastic-kind collisions occur when neutrons collide with the formation of mineral nuclei. When neutrons collide with an object of equal mass, such as a hydrogen atom, they lose the greatest energy. The neutrons enter the thermal state and lose significant amounts of charge within a few microseconds after being emitted. Neutrons are caught by various atoms' nuclei when in the thermal state (Cl, H, B). The atom that successfully absorbs the neutron experiences intense excitement and releases a gamma ray.

1.3 Standard Model of Particle Physics and Lifetime of Neutron

The Standard Model of Particle Physics is a theoretical framework that describes the fundamental particles and their interactions using three of the four fundamental forces: electromagnetism, weak nuclear force, and strong nuclear force. It divides all particles into two major categories:

fermions, which include quarks and leptons, and bosons, which include force-carrying particles like photons and W and Z bosons. In nuclear and particle physics, the lifetime of a neutron is an essential concept. When unbound from an atomic nucleus, free neutrons decay after a mean lifetime of around 15 minutes and 49 seconds, or 880 seconds. The process of neutron decay usually results in the following three states: proton, electron (beta particle), and electron antineutrino. The precise value of the neutron lifetime has been measured experimentally with high precision, and its value is essential for understanding various aspects of nuclear physics, cosmology, and particle physics.

The formula for the Hamiltonian of neutron decay is:

$$\mathrm{M} = \left[\mathrm{G_v}\mathbf{p}\gamma_\mu \mathrm{n} - \mathrm{G_A}\mathbf{p}\gamma_5\gamma_\mu \mathrm{n}\right]\left[\mathbf{e}\gamma_\mu(1+\gamma_5)\mathrm{v}\right]. \qquad (1)$$

where **p**, n, **e**, and v are the relativistic spin wave functions of the proton, neutron, electron, and antineutrino. This Hamiltonian break parity symmetry is a significant and distinct characteristic of the weak interaction since it involves both vector (G_V) and axial vector (G_A) couplings.

Using Fermi's golden rule, one can calculate the probability of neutron decay per unit of time from the Hamiltonian, Equation (1):

$$\mathrm{dW} = (2\pi)^{-5}\,\delta(\mathrm{E_e} + \mathrm{E_v} - \Delta)\frac{1}{2\mathrm{E_e}}\frac{1}{2\mathrm{E_v}}\mathrm{d}^3\mathbf{p_e}\mathrm{d}^3\mathbf{p_v}|\mathrm{M}|^2. \qquad (2)$$

Here E_e, $\mathbf{p}_e$, E_v, and $\mathbf{p}_v$ are the electron and antineutrino total energy and momentum and Δ are the neutron-proton mass difference: Δ = 1.29333205(51) MeV. The beta electron energy spectrum is obtained by integrating Equation (2) over the antineutrino and electron momenta:

$$\frac{\mathrm{dW}}{\mathrm{dE_e}} = \frac{\mathrm{G_V^2}+3\mathrm{G_A^2}}{2\pi^3}\mathrm{E_e}|\mathbf{p_e}|(\Delta - \mathrm{E_e})^2. \qquad (3)$$

The exponential decay rate constant is obtained by doing an extra integration over electron energy:

$$\mathrm{W} = \frac{\mathrm{G_V^2}+3\mathrm{G_A^2}}{2\pi^3}\mathrm{f_R}. \qquad (4)$$

The value of the integral throughout the Fermi energy spectrum, taking along the radiative, recoil order, and Coulomb corrections, is represented by the symbol f_R. The neutron lifetime τ_n is the inverse of W:

$$\tau_\mathrm{n} = \frac{2\pi^3}{(\mathrm{G_V^2}+3\mathrm{G_A^2})\mathrm{f_R}}. \qquad (5)$$

In natural units, or writing the physical constants explicitly, this becomes:

$$\tau_n = \frac{2\pi^3\hbar^7}{(G_V^2+3G_A^2)m_e^5c^4f_R}. \qquad (6)$$

Some corrections are required to this quantity. Effects of the order of recoil (Emax/Mn ≈ 8×10^{-4}) include induced hadronic currents, especially weak magnetism, which can be calculated from the magnetic dipole moments of the neutron and proton, as was especially demonstrated using the conservation of vector current (CVC) hypothesis. Traditionally, outer, and inner corrections are distinguished in radiative corrections. The long-range electromagnetic corrections for both actual (bremsstrahlung) and virtual photons, comprising the infrared divergence and Coulomb adjustments to the electron wave function, constitute the outer corrections, accounting for approximately 1.5% of the neutron lifetime. Model-dependent short-range electroweak adjustments make for around 2% of the inner corrections. Marciano and Sirlin discover revised values for these adjustments.

$$\tau_n = \frac{G_F^2}{(G_V^2+3G_A^2)} 4908.7(1.9)\text{s}. \qquad (7)$$

where G_F = 1.1663787(6) × 10^{-5} GeV^{-2} is the Fermi weak coupling constant calculated from the muon decay lifetime [1].

1.4 The Lifetime of the Neutron and Big Bang Nucleosynthesis

The lifetime of the neutron plays a crucial role in the process of Big Bang nucleosynthesis (BBN), which is the formation of light atomic nuclei in the early universe. During the first few minutes after the Big Bang, the universe was extremely hot and dense, and nuclear reactions occurred rapidly. Experimental measurements of the neutron lifetime help constrain the predictions of Big Bang nucleosynthesis models and refine our understanding of the early universe. By comparing the predicted abundances of light elements (such as hydrogen, helium, and lithium) from Big Bang nucleosynthesis models with observations of the initial abundances in the universe, scientists can test the consistency of the Standard Model and explore for any potential deviations or new physics beyond our current understanding. Therefore, the neutron lifetime is a critical parameter in our understanding of particle physics and cosmology.

The process by which atomic nuclei containing multiple nucleons were created in the early universe. The three nuclear processes were able to maintain the proton-to-neutron ratio at about 1:1.

$$n + e^{+} \leftrightarrow p + \boldsymbol{\nu}_e$$

$$p + e^{-} \leftrightarrow n + \boldsymbol{\nu}_e$$

$$n \leftrightarrow p + e^{-} + \boldsymbol{\nu}_e$$

The first two of these nuclear reactions occurred in both time order in the early universe. Nuclear processes began to favour the creation of protons over neutrons as the cosmos cooled.

The universe's temperature lowered to the point shortly after the Big Bang that the first two nuclear reactions were effectively "frozen". The ratio of protons to neutrons was around 6 to 1. The universe's temperature continued to drop over the following 200 seconds, and heavier nuclei started to form. Some of the neutrons go through decay over these about 200 seconds, creating additional protons. The proton-neutron ratio went from 6:1 to 7:1 because of these decays. The fraction of heavy nuclei created after about 200 seconds depends on the precise ratio of protons and neutrons present at this time. According to BBN theory, around 75% of the baryons were still free protons, about 25% bound to 4He nuclei, and the remaining few baryons formed traces of 2H, 3He and A > 4 nuclei. All Baryon densities have an impact on BBN estimations of mass fractions of various nuclei and neutron lifetimes in the early universe [21].

The neutron decay parameters, such as the lifetime of the neutron and the strength of the weak nuclear force responsible for neutron decay, are directly related to the neutron-to-proton ratio during nucleosynthesis processes, including Big Bang nucleosynthesis (BBN). Since neutrons decay into protons with a relatively short lifetime, the rate of neutron decay directly affects the neutron-to-proton ratio. A shorter neutron lifetime would mean more rapid decay of neutrons into protons, leading to a decrease in the neutron-to-proton ratio. Conversely, a longer neutron lifetime would allow more time for neutrons to participate in nuclear reactions before decaying, increasing the neutron-to-proton ratio. The neutron-to-proton ratio during nucleosynthesis is

crucial because it determines the abundance of heavier elements produced. Neutrons are necessary for the formation of heavier isotopes through neutron capture reactions. Therefore, understanding the neutron decay parameters is essential for accurately modelling the nucleosynthesis processes and predicting the observed abundances of light elements in the universe.

Chapter 2

Theory and Motivation

2.1 Fundamentals and Concepts

Neutrons are one of the fundamental particles in the universe, along with protons and electrons. They play a crucial role in the structure of atomic nuclei and are essential for nuclear reactions and processes such as nuclear fission and fusion. Neutrons do not survive for a very long time outside the nucleus, like many other subatomic particles. In around fifteen minutes, it breaks down into protons, electrons, and tiny particles known as antineutrinos. However, the rate at which a neutron decay is not well understood. A measurement of 887.7 ± 2.2 seconds was made using one method. Another approach provides a measurement of 878.5 ± 0.8 seconds. This variation initially appeared to be a problem with measurement sensitivity. However, differences continue as researchers carry out more exacting tests to identify potential issues. Physicists require more precise neutron lifetime data to calculate the relative abundances of hydrogen and helium produced in the first few minutes of the universe.

2.2 Detecting Protons from Neutrons Decay

Due to the challenges of detecting neutrons directly, silicon detectors are used for the detection of protons from neutron decay. After accelerating the decay protons that leave the trap in an electrostatic potential to an energy of 35 keV, the protons are detected with a silicon detector with (necessarily) a 500nm metallization and dead layer. One of the systematic uncertainties in this type of experiment is proton backscattering. This is difficult to measure because these protons are backscattered by the detector and often leave no signal on the detector. It is also difficult to model because it can depend on the crystal structure of silicon. The backscattering probability depends on the silicon detector's metallization layer as well as the dead layer's thickness.

2.3 Why Neutron Lifetime is Important?

The neutron lifetime is an important parameter in both nuclear physics and cosmology. Precise measurements of the neutron lifetime serve as tests of theoretical models in particle physics. The Standard Model of particle physics predicts the neutron lifetime based on the strength of the weak nuclear force, which governs neutron decay. Experimental measurements of the neutron lifetime provide constraints on the parameters of the Standard Model and help test its validity.

If we know the rate of neutron decay, we can find out how weak forces impact other particles. The weak force plays a crucial role in the decay of neutrons into protons, electrons, and electron antineutrinos, as well as in certain processes involving protons. In beta decay, a down quark within a neutron transforms into an up quark, emitting a W^- boson, which then decays into an electron and an electron antineutrino. This process changes the flavour of the quarks within the nucleons and converts a neutron into a proton. Overall, the weak force governs a variety of interactions among particles, influencing processes ranging from radioactive decay and neutrino interactions to nuclear reactions and particle decay. Understanding these weak interactions is crucial for describing the behaviour of particles and the fundamental forces that govern their interactions.

The cosmic ratio of helium to hydrogen, as well as the proportions of deuterium and other light elements, may be determined using astronomical data. It would be interesting if these observations corroborated the results as expected by the Big Bang hypothesis. We may compare the observed ratio from astrophysical experiments with the expected value from theory once the neutron lifetime is adequately understood.

Researchers in multiple other teams throughout the world are working on different strategies to estimate the neutron lifetime along with continuing the beam and bottle tests. A group is developing a brand-new beam experiment at the Japan Proton Accelerator Research Complex (J-

PARC) in Tokai that will concentrate on detecting the electrons released when neutrons decay rather than the protons. Neutron bottles, which will employ magnetic fields rather than material boundaries to contain ultracold neutrons, are another interesting development. These teams include those at the Los Alamos National Laboratory, the Petersburg Nuclear Physics Institute in Russia, the Technical University of Munich, and the Johannes Gutenberg University Mainz in Germany.

2.4 The Lifetime of Neutrons in Space

For the first time, scientists have taken neutron lifetime measurements in space. Some neutrons are released into space when cosmic rays, which are always moving through space, strike with atoms on the surface of a planet or in its atmosphere. These neutrons are released into space until they disintegrate [3]. In theory, elevated altitudes should exhibit a lower neutron count; however, accurate measurements necessitate the use of appropriate tools at the correct altitude.

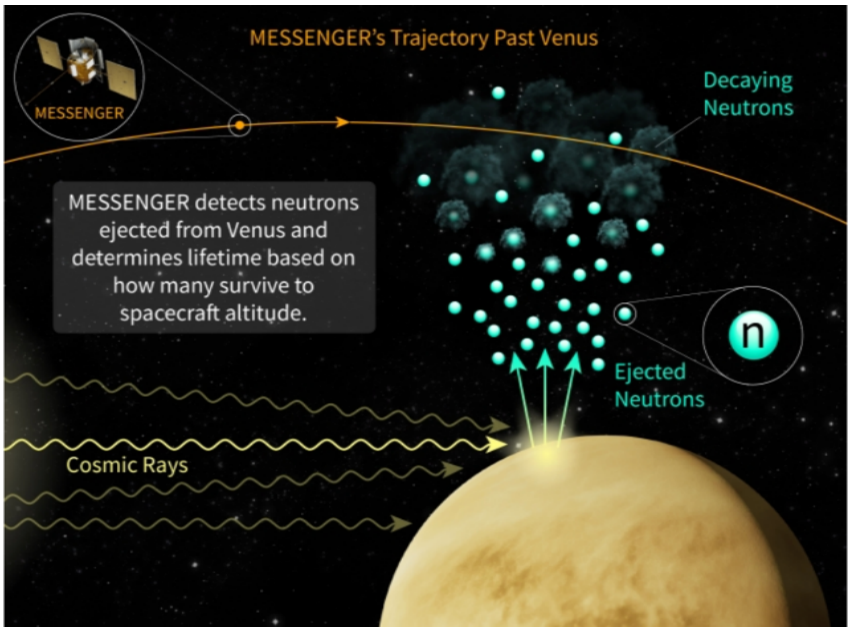

Figure 2. 1 The lifetime of a neutron in space [3].

NASA's Mercury Surface, Space Environment, Geochemistry, and Ranging (MESSENGER) probe orbited Mercury in a complex path between 2011 and 2015. The neutron spectrometer on MESSENGER's spacecraft gathered information on the planet's fast-moving neutrons as it travelled Venus [3].

The MESSENGER's orbit was about as far as these neutrons could go before disintegrating at its lowest altitude of 339 kilometres (210 miles). Similar measurements were taken at a minimum altitude of 205 kilometres during a flyby of Mercury (127 miles).

2.5 Cabibbo-Kobayashi-Maskawa (CKM) and Neutron Decay

The Cabibbo-Kobayashi-Maskawa (CKM) matrix is a unitary matrix in the Standard Model of particle physics that describes the mixing between the three generations of quarks: up, down, charm, strange, top, and bottom.

One application of the CKM matrix is in the study of neutron decay. In neutron decay, a neutron (which is made up of two down quarks and one up quark) decays into a proton, an electron, and an antineutrino. This process involves weak interaction, which is mediated by the exchange of W and Z bosons. The CKM matrix comes into play because the weak interaction involves mixing the quark flavour states. In neutron decay, one of the down quarks in the neutron is transformed into an up quark, producing a proton. By assuming that both the neutron and the proton are point-like Dirac particles that pair directly to a W−, a first approximation to neutron beta decay can be obtained. Figure 2.2 illustrates the four-fermion Feynman diagram using this approach [23].

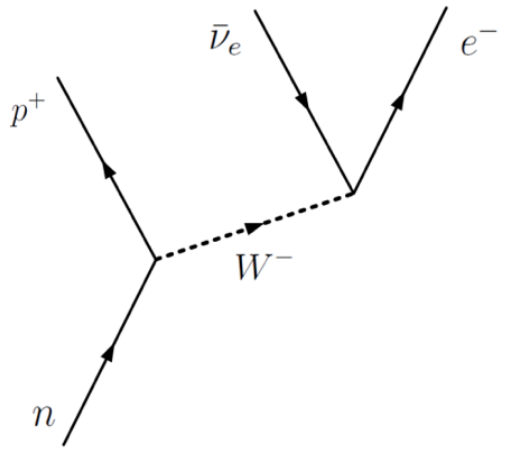

Figure 2. 2 Neutron Decay assuming a point like proton and neutron [23]

The probability of neutron decay depends on the value of |Vud|. Experimental measurements of neutron decay provide a way to determine the value of this CKM matrix element, which is important for testing the Standard Model and searching for new physics beyond it.

It is necessary to experiment to measure the survival rate or the decay rate through the neutron's decay products to determine the neutron's lifetime. The neutrons that are still present after encasing ultra-cold neutrons (UCNs) in a magnetic, gravitational, or material container can be counted using one technique. Neutrons having kinetic energy under 0.2 eV are known as UCNs. Either a UCN bottle or a cold neutron beam can be used to calculate the decay rate.

Due to differences between the quarks' mass eigenstates and the weak eigenstates involved in the decay process, the neutron's decay rate is somewhat reduced. The linear fusion of many weak eigenstates results in the down quark mass eigenstate in the neutron. This mixing is governed by the Cabibbo-Kobayashi-Maskawa (CKM) matrix, which is seen below.

$$\begin{pmatrix} d \\ s \\ b \end{pmatrix}_{\text{weak}} = \begin{pmatrix} V_{ud} & V_{us} & V_{ub} \\ V_{cd} & V_{cs} & V_{cb} \\ V_{td} & V_{ts} & V_{tb} \end{pmatrix}_{\text{CKM}} \begin{pmatrix} d \\ s \\ b \end{pmatrix}_{\text{mass}}$$

When measurements of the unitary CKM matrix indicate a substantial deviation from unitarity, it serves as an illustration of fundamental principles in physics. Neutron decay may be extended to include exotic contact interactions, scalar/tensor interactions from Higgs or supersymmetric particles, and several other novel physics models:

$$V_{ud} \sim V_{cs} \sim \cos(\theta c)\,; V_{us} \sim -V_{cd} \sim \sin(\theta c).$$

Considering if SM is correct and that there can be only three generations of quarks, the nine components of the CKM matrix can only be defined regarding four real parameters, the third and fourth of which may each be actual angles. CP symmetry is broken if this phase does not constitute an integral multiple. There must be at least three generations of quarks for this to be feasible. The unitarity of the CKM matrix demands that given the current situation,

$$|V_{ud}|^2 + |V_{us}|^2 + |V_{ub}|^2 = 1,$$

and the significance of neutron decay lies in identifying the greatest matrix element V_{ud}.

2.6 Neutron Lifetime Observations from the Past

There are two methods to measure the neutron lifetime, the beam method and the bottle method and the main goal of BL3 is to explore and assess the systematic results of the beam method to resolve the discrepancy between beam-type and bottle-type measurement of neutron lifetime.

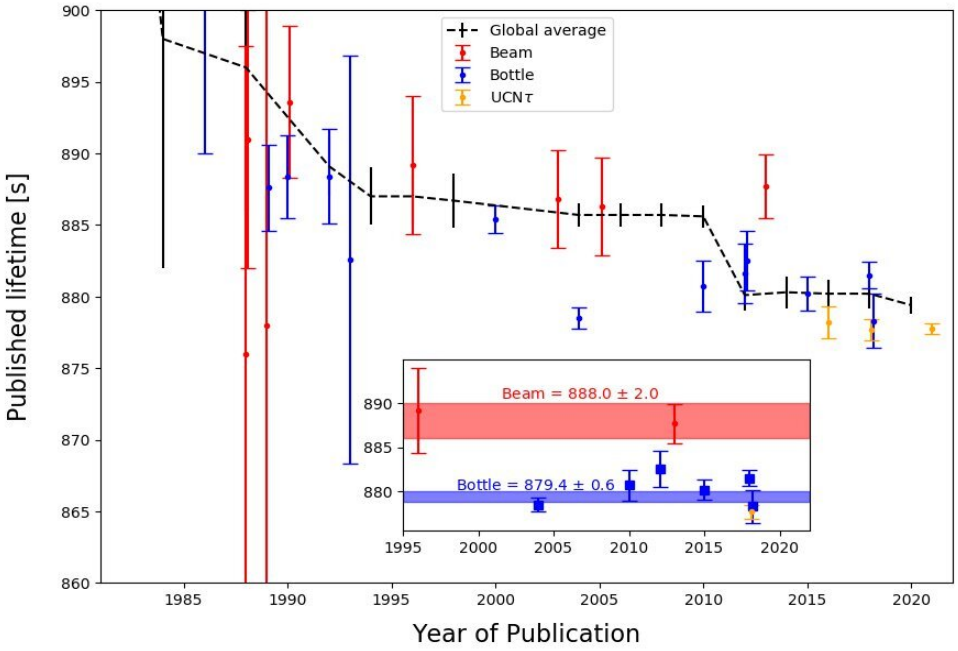

Figure 2. 3 Comparison of Neutron lifetime results from several experiments [4].

The figure shows the comparison of neutron lifetime results from several experiments performed since the early 1980s. Results differ by multiple standard deviations in the uncertainty. Beam experiments are shown in red, and bottle experiments are in blue. The UCNtau project's recent results, which are the most precise yet, are shown in yellow and indicate a neutron lifetime of 877.75 seconds with an uncertainty of 0.34 seconds [4].

- In the bottle technique, neutrons are trapped in a container, and the quantity left is counted after a predetermined time. In the beam technique, Neutron streams are produced by the apparatus used in beam experiments. Scientists count the neutrons inside a given beam volume. Then they send the stream through a magnetic field and into a particle trap formed by an electric and magnetic field. Neutrons decay in the trap where scientists measure the number of protons left.
- Beam experiments and bottle experiments often have different experimental conditions. For instance, in beam experiments, particles are typically produced at higher energies and may have different energy spectra compared to particles in bottle experiments. These differences in energy and particle flux can lead to variations in the observed phenomena.

- Different experimental setups may introduce different systematic errors. For example, in bottle experiments, uncertainties in neutron trapping and detection efficiency, background radiation, and environmental effects can contribute to systematic uncertainties in measurements. Beam experiments may have their own set of systematic errors related to beam properties, target interactions, or detector response. The techniques used to detect and analyze particles may differ between beam and bottle experiments. This can lead to variations in the sensitivity, resolution, and accuracy of measurements. In both types of experiments, statistical fluctuations can occur due to the finite number of events or measurements. These fluctuations can lead to variations in the measured quantities, particularly in experiments with low event rates or short observation times.
- Beam and bottle experiments can provide valuable insights into particle physics, differences in experimental conditions, systematic errors, detection techniques, and statistical fluctuations can contribute to potential discrepancies in measurements between the two types of experiments. Scientists carefully analyze and compare results from different experimental setups to understand discrepancies.

2.7 Description of Beam Technique

There are two substantially different methods for determining neutron lifetimes. The first strategy is founded on the detection of β-decay products (protons or electrons) during the passage of the neutron beam through the experimental setup. Different physical quantities are measured using these two techniques. The second technique, on the other hand, enables the use of the neutron number to determine the overall decay probability without regard to the particle's ultimate state or the decay channel.

Beam technology measures lifetime by counting the absolute number of protons in a reference volume while continuously monitoring the absolute neutron flux. Byrne et al. were the ones who originally suggested using proton trapping to increase the signal-to-noise ratio [5]. The whole neutron beam is contained inside a trapping zone of length L. By looking for decaying neutrons

inside this area's volume, neutron decay is seen with efficiency ε_p. A velocity-dependent fluence rate I(v) is a defining characteristic of a neutron beam. The average amount of neutrons in the trap at any given time can be calculated by:

$$N_n = L\int_A da\, I(v)\frac{1}{v},$$

where A is the trap cross-sectional area having non-zero fluence. Thus, the rate at which decay events are detected, N_p, is:

$$N_p = \tau^{-1}\varepsilon_p L\int_A da\, I(v)\frac{1}{v},$$

After leaving the trap, the neutron beam passes through a detector whose efficiency of detecting low-energy neutrons is proportional to 1/v [5].

To conduct studies using the beam approach, precise measurements of the starting neutron flux and the number of protons is needed. This is because the outcome depends on the proportion between these two factors.

2.8 The Equation for Neutron Lifetime Using Beam Method

The earliest beam technique for finding the neutron lifetime counts final state charged particles, calculates neutron flux, and calculates the effective decay volume to determine the beam's specific activity and radioactive decay constant. The systematic constraints of the neutron flux measurement were the main constraint on the most recent beam neutron lifetime experiment, which only managed to obtain an experimental error of 3.4 seconds. The figure below illustrates the key components of a beam neutron lifetime measurement, which involves passing a collimated slow neutron beam through a known decay volume. The neutron beam is typically produced by a research reactor or spallation neutron source.

One or more charged particle detectors which measure the neutron beta decay's end-state protons or electrons (or both) look at the decayed area [6]. Early beam lifetime studies observed

both in coincidence to lower background, while more modern experiments only count protons to improve accuracy in calculating the effective decay volume and counting efficiency. As the beam travels through, a tiny piece of absorbing foil is used to constantly measure the neutron flow.

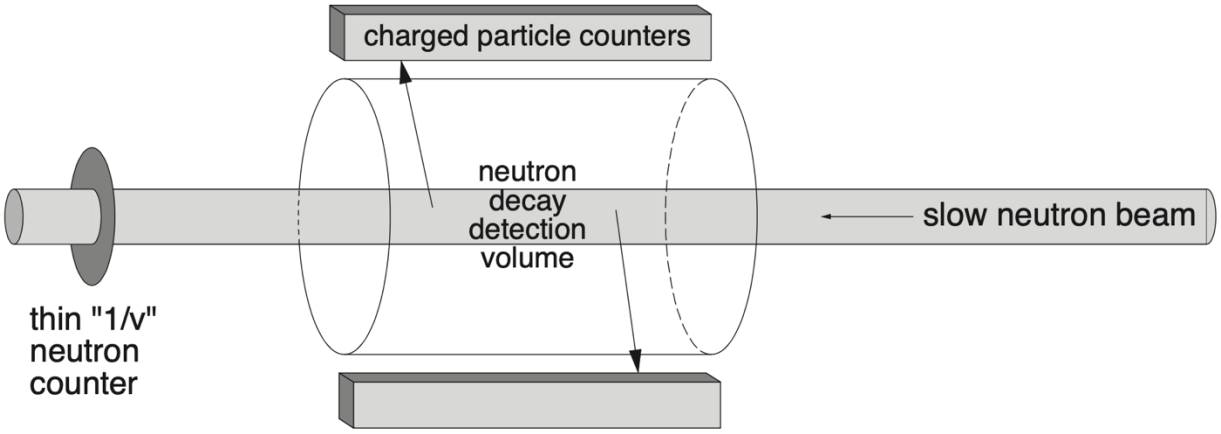

Figure 2. 4 The fundamental design of a beam neutron lifetime experiment [6].

The differential equation that describes the neutron decay rate (Γ) in the decay region is:

$$\Gamma = -\frac{dN}{dt} = \frac{N}{\tau_n}, \qquad (1)$$

where N is the number of neutrons and τ_n is the neutron lifetime, which is the average time it takes for a neutron to decay. This equation expresses the decay constant (Γ) in terms of the neutron lifetime (τ_n):

$$\mathrm{N} = \rho_\mathrm{n} \mathrm{V}_\mathrm{det} = \left(\frac{\varphi_\mathrm{n}}{\mathrm{v}_\mathrm{n}}\right) \mathrm{A}_\mathrm{beam} \mathrm{L}_\mathrm{det}. \qquad (2)$$

The average density of neutrons (ρ_n) can be defined as the quotient of the average neutron flux (ϕ_n) and the velocity of neutrons (v_n), while V_{det} represents the volume used for detection. If we assume that the latter is sufficiently large to cover the entire cross-sectional area of the beam (A_{beam}), then we substitute V_{det} with the product of A_{beam} and the length of the decay region (L_{det}).

A neutron lifetime equation for a monochromatic (single velocity v_n) neutron beam can be obtained by merging Equations 1 and 2:

$$\tau_n = \frac{A_{beam} L_{det}}{\Gamma(\frac{\phi_n}{v_n})} . \quad (3)$$

while an integral of the spectral flux $\phi_n(v)$ is given by:

$$\tau_n = \frac{A_{beam} L_{det}}{\Gamma \int \frac{(\varphi_n(v))}{vdv}}. \quad (4)$$

The measured neutron decay rate R_p is because the neutron decay detector measures the decay particles (such as protons) with efficiency ε_p:

$$R_p = \varepsilon_p \Gamma , \quad (5)$$

and

$$\sigma_{abs} = \frac{\sigma_{th} v_{th}}{v} , \quad (6)$$

where v_{th} is the reference thermal neutron velocity. The flux monitor count rate R_n is given by:

$$R_n = \varepsilon_{th} A_{beam} v_{th} \int \frac{\varphi_n(v)}{vdv} . \quad (7)$$

We derive an equation for the neutron lifetime in terms of experimentally determined values by combining Equations 4, 5, and 7 we get [23]:

$$\tau_n = \frac{R_n \varepsilon_p L_{det}}{R_p \varepsilon_{th} v_{th}} . \quad (8)$$

2.9 Description of Bottle Technique and Ultracold Neutrons

Neutrons that are extremely cold move significantly more slowly than ordinary ones. 10 million metres per second for fission processes vs a few metres per second. In the beginning and after some time, scientists count the neutrons in the container. This difference allows us to determine how quickly a neutron decays.

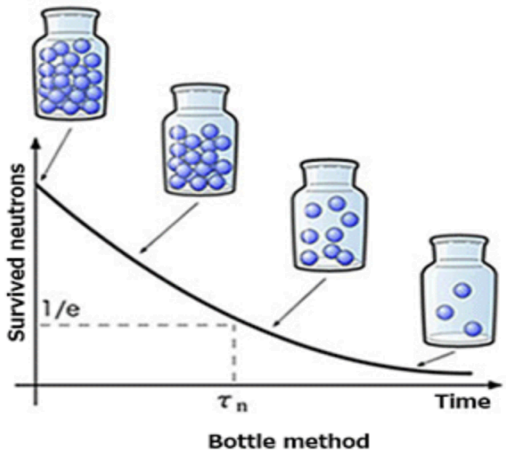

Figure 2. 5 An image of the bottle technique [11].

The bottle experiments that physicists were working on had their challenges. Preventing the loss of neutrons due to contact with the container material was one of the toughest hurdles. Calculations of lifetime are thrown off by leakage because it changes the neutron count. Researchers can lessen the uncertainty of this important parameter thanks to an improved version of the "bottle" experiment, but an important conflict still exists.

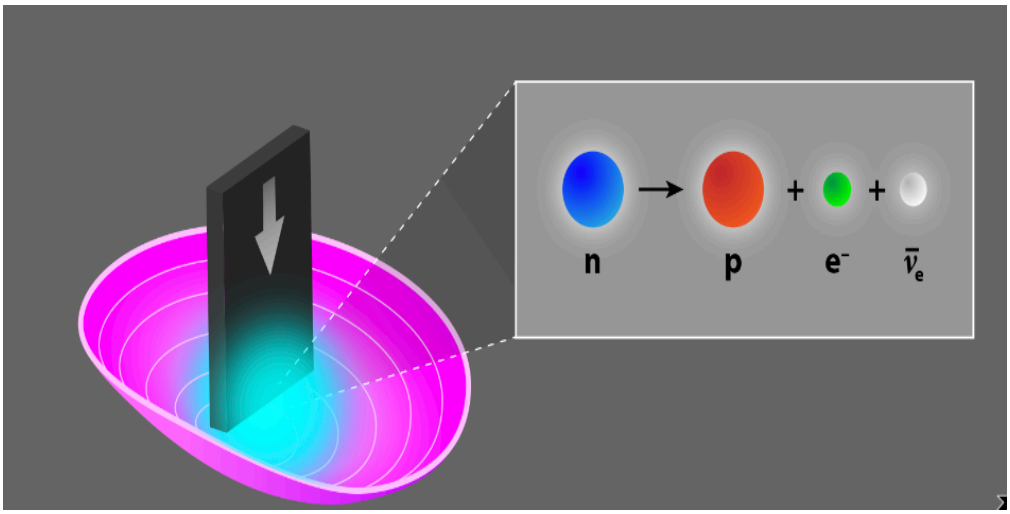

Figure 2. 6 This is an experimental image of the UCNτ collaboration [12].

Cryogenic neutrons are trapped in a magnetic gravity trap for a predetermined amount of time. Some neutrons experience beta decay during this period. The detector (a grey sheet) is dropped

into the trap after the period to count the leftover neutrons. So, the bottle and storage neutrons have their decay product over time monitored.

In the bottle experiment, cryogenic neutrons (UCN) are stored in bottles for varying periods and the remaining UCN in the bottles are counted after the storage time. The number of UCNs that do not decay during storage is modelled as follows:

$$< N(t) >= N_0 e^{-\frac{t}{\tau}}$$

where N_0 is the number of UCN in the bottle at time t = 0.

Two iterations of this experiment were performed with different hold lengths (short hold length t_S and long hold length t_L), and the number of UCNs remaining in the bottle at the end of the iteration was $N(t_S) = N_S$, where N was $(t_L) = N_L$, the lifetime can be extracted as:

$$\tau = \frac{t_L - t_S}{ln\frac{N_S/N_0}{N_L/N_0}} = \frac{t_L - t_S}{ln\frac{N_S}{N_L}}.$$

The fact that UCNs are neutrons that may be kept in a container is one of their characteristics. Strong interactions with the wall's constituent nuclei are the main way that UCNs and physical walls interact.

Cryogenic neutrons (UCN) have very low energies, less than 300 neV. We can detect potentials attainable in the laboratory for magnetic, gravitational, and matter-related aspects at these energy levels. The UCN has a wavelength of more than 500 angstroms, a temperature of less than 4 mK, and a velocity of fewer than 8 m/s. Strong magnetic fields of roughly 6 Tesla can polarise them, and materials like nickel and copper can reflect them.

The parameters of the nucleon charge weak current are extremely precisely determined by angular correlation measurements in neutron beta decay, neutron lifetime, and radioactive decay studies. Some of these characteristics, notably the nucleon axial coupling constant, have a

clear parameter in neutron decay. This is significant for limits on different extensions of the standard model of particle physics as well as high-precision estimations of the solar fusion rate and neutrino flux.

Neutrons at lower temperatures, located within the material, scattered, giving up nearly all their energy to become UCN. At the same time, the opposite process of UCN up scattering is suppressed by lowering the temperature of the moderator as shown below [7].

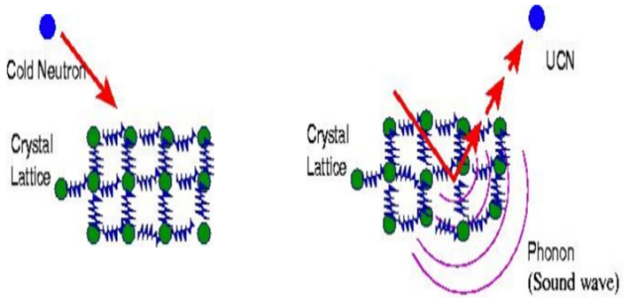

Figure 2. 7 The opposite process of UCN up scattering [7].

The beta asymmetry, or the relationship between decaying beta particles and neutron spins, is measured by UCNA. To create decay geometries that are competitive with those of traditional cold neutron beam experiments, UCNA makes use of the characteristics of UCN. The neutron production background generated by UCNs stored in beta decay detectors is extremely low, especially when paired with the detector geometry for UCNA studies.

The experiment that is related to ultra-cold neutrons is in process at Nab. In the Nab experiment, protons and electrons are simultaneously detected from unpolarized cold neutron decay at Oak Ridge National Laboratory's SNS facility. A dedicated silicon particle detector for the Nab experiment will be designed and assembled at LANL (Los Alamos National Laboratory) and tested at the LANSCE (Los Alamos Neutron Science Center) UCN facility using neutron and superconducting magnets.

UCNτ uses magnetic traps to confine neutrons and prevent them from interacting with the material surface during storage. A 670-litre magnetic trap consisting of more than 5,000 NdFeB

magnets (the largest of its kind) was successfully commissioned in early 2013 to investigate new UCN detection methods to further improve previous measurements. Development is in progress.

The compact beta calorimeter and ultracold neutron storage cell are merged into one tiny unit for the UCNb experiment. To acquire the desired neutron density in the cell, the experiment is positioned as closely as possible to the powerful light source LANSCE UCN [7].

Chapter 3

Experimental Setup

3.1 Measurements Involved in Neutron Lifetime

Neutron lifetime can be determined using either one of two methods: the beam technique or the bottle approach. The easiest approach to ensure accurate measurements is to measure the same quantity using two or more different techniques. By taking measurements before and after a neutron decays, scientists have discovered a method to determine lifetimes. Both approaches became better over time, but they still can't be compared.

3.1.1 Beam Method

The beam technique, which was invented by Robson in 1951 and was first applied at the NRX reactor in Chalk River, Canada, is the earliest method for determining neutron lifetimes. A known detection volume V is traversed by a slow (hot or cool) neutron beam. The differential version of the radioactive decay equation determines the neutron decay rate in this volume:

$$\Gamma = -\frac{dN}{dt} = \frac{N}{\tau_n},$$

where Γ_n is the neutron lifetime and *N* is the number of neutrons in the detection volume, which can be found from the neutron flux φ and velocity *v* and is given by:

$$N = \frac{\varphi V}{v}.$$

One of the most important aspects of many neutron lifetime investigations is that the flux is defined by the reaction rate of neutrons absorbed by a thin foil with an absorption cross-section that is inversely proportional to the neutron velocity. For most neutron absorbers, this is a reasonable estimate.

Equipment that produces a neutron stream is used in beam experiments. Scientists count the neutrons that are present in a certain area of the beam. The magnetic field and electric field combine to create a particle trap, which is subsequently filled with an electric current. Scientists count the remaining protons after neutrons decay within the trap. Accurate measurement is especially challenging with beam experiments. Two absolute measurements are needed for beam measurements as opposed to only one.

In the beam technique, a segmented proton trap is entered by a cold neutron beam. The 4.6 T magnetic field and electrostatic potential at each end of the trap capture the proton as it decays from the neutron. The centre electrode receives a ramp voltage while the upstream electrode is periodically depressed to force every proton out of the trap. The protons travel along magnetic field lines from the direct beam and are accelerated and detected by a silicon detector that is kept at a high potential. While this process is repeated, a downstream neutron flux metre continuously monitors the neutron beam.

Table 1 Systematic and statistical uncertainties for NIST beam neutron lifetime experiment [8].

Source of uncertainty	Previous (s)	Phase II (s)	Phase III (s)
Neutron flux detector efficiency	2.7	0.5	< 0.1
Abs/scatt in ^{6}LiF deposit and Si substrate	0.9	0.3	< 0.1
Neutron beam halo	1.0	0.1	< 0.1
Proton trap nonlinearity	0.8	0.2	< 0.1
Proton backscatter correction	0.4	0.4	< 0.1
Counting statistics	1.2	0.6	< 0.1
Quadrature sum	**3.4**	**1.0**	**0.1**

Column 1 of the prior NIST beam neutron lifetime experiment's systematic and statistical errors are listed in seconds. This information was taken from Nico et al (2005). In the next two columns, Phases II and III should improve [8].

Therefore, in a broad sense, we may say that the beam distributes neutrons to a certain region to count the decay products and determine the loss rate.

3.1.1.1 Counting Proton

Protons are detected using silicon detectors and proton traps, which have a circular electrostatic trap with sixteen electrodes split along the beam ray and a 4.6 T magnetic field along the beam axis [9]. Because these electrodes form a potential well per volume of neutron beam at a depth of around +800 eV, which is significantly higher than the maximum kinetic energy of protons, which is 751 eV, protons are only permitted to flow vertically in the trap mode. Since the protons' maximum cyclotron radius in the 4.6 T field is less than 1 mm, the protons from neutron decay are likewise radially constrained. Apart from the ends of the trap, where potential gradients impact the efficiency, the protons from neutron decay are therefore captured with unit efficiency. The trapped protons are freed from the trap and adiabatically steered along the magnetic field lines that bend them away from the neutron beam before being shot into a detector located at a strong negative potential after being locked up for a period of 10 ms.

3.1.1.2 Proton Tracking

More knowledge has been gained about most of the remaining substantial systematic effects and proton count uncertainties since the Lifetime Instrument was last used, around 20 years ago. For instance, simulations revealed that the magnetic field gradient was too strong for the longest trap length, which was employed in the 2001 dataset. For an error of 0.8 seconds, a correction of 5.3 seconds was required. Using a superconducting solenoid and proton detector setup that was calculated with the GEANT4 and MCNP packages as well as specially generated code, radioactive neutron decay was quantified in two of his subsequent tests. As a result, one's understanding of geometry, particle motion, and magnetic and electrostatic fields has increased [9].

Radiation decay studies show that proton detectors can function at high voltages with larger areas (600 mm^2 vs 300 mm^2) and thicker (1.5 mm vs 0.3 mm) silicon detectors. We can study

and lessen the likelihood of protons being lost because of neutron halos with a bigger region. Outside of the silicon active zone, neutrons collide as they decay and go to the detector.

The initial positions of protons were used as inputs for GEANT4 simulations of past radiation decay experiments using magnetic and electric fields. These simulations looked at how various detector configurations, dead layer materials (Au, Si), and dead layer thicknesses impact the efficiency of proton detection. Since GEANT4 can track protons after backscattering, it offers an advantage over prior SRIM estimates of proton backscattering. This feature makes it possible to calculate the proportion of protons for each detector configuration that does not return to the active zone.

The Mark III proton trap is a tested improvement to the original concept. Two trap electrode stacks are shown in the image below [9]. The old trap (also known as the "Mark II") consists of a stack of gold-plated fused silica trapping electrodes with a fused silica spacer in between each electrode. The stack is held together by the axial compression of the two end plates. By holding each electrode separately in a kinematic mount and supporting the entire structure in a stainless-steel frame, the Mark III trap does away with the need for spacers. The Mark III trap provides benefits in terms of enhanced trap volume pumping, increased inner electrode surface quality, and simpler measuring processes for finished traps.

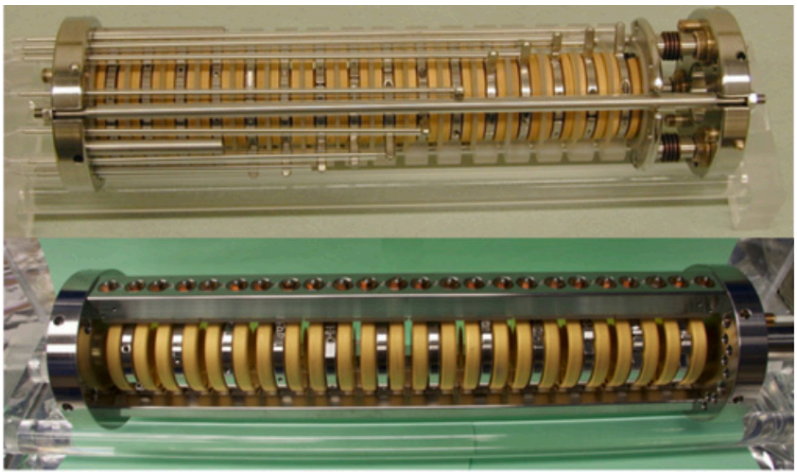

Figure 3. 1 Images of the mark II (top) and mark III (bottom) electrode stacks for the traps [9].

3.1.1.3 Proton Detector

The released protons from the trap were located using a passivated ion implantation planar detector and a silicon surface barrier detector. For protons with incidence energies greater than 20 keV, they offer remarkable energy resolution and good detection effectiveness. To lower detector capacity, choose the lowest area detector that entirely encloses all protons coming from the trap. Therefore, a detector with a 300 mm^2 effective area and a 300 m depth is used. To reduce the impacts of preamplifier noise and detector leakage current, Light energy was used to cool the detector and preamplifier to a temperature of about 150 K.

Low-energy protons must be accelerated to a significantly negative potential to be seen by the detector. All silicon detectors have an inert layer, sometimes referred to as the inert layer, on their surface. Depending on the silicon detector type being utilized, this layer could be comprised of silicon dioxide or gold. The proton recoil energy from neutron decay is so minimal that it cannot penetrate dead layers without additional acceleration (up to 751 eV). Typical accelerating voltages for this experiment varied from -25 to -35 kV. To prevent collecting electrons in the decaying area, it decided to run the proton detector at a high voltage rather than trapping it at a high positive potential.

3.1.1.4 Orientation of Proton Detector

Three different techniques were utilized by scientists to make sure the proton detector was exactly centred in the proton beam produced by the trap since it was crucial to position it there. Theodolite surveying, source centroid measurement, and centroid measurement of protons from neutron decay are part of them.

The proton trap was initially positioned parallel to the neutron beam and then firmly fastened to the inside bore of the magnet. To align the trap, crosshairs were put into their downstream and upstream ends. The survey target operated inside the magnet bore was centred on the detector and was equipped with a linear motion feedthrough with a 1 m range of motion. Using a mirror that was put into the magnet bore, the alignment axis was fixed at 9.5 degrees concerning the

beam. In the second method, an electron source was placed within the trap's downstream electrode.

The most accurate confirmation of the detector's position comes from the decay protons. Despite being without a doubt the most crucial alignment indication, the test takes longer because the event rate is much lower (in comparison to the electron source). Due to the lower count rate, no mask is used, but the measurement procedure is the same as when utilizing an electron source. By fitting the data to the point where a square distribution and a Gaussian function converge, the centroid may be found. The image below displays the scan for one detector's motion direction [10]. The ratio of proton to neutron rate vs detector position is the essential variable to plot to prevent proton rate drifts caused by reactor power changes.

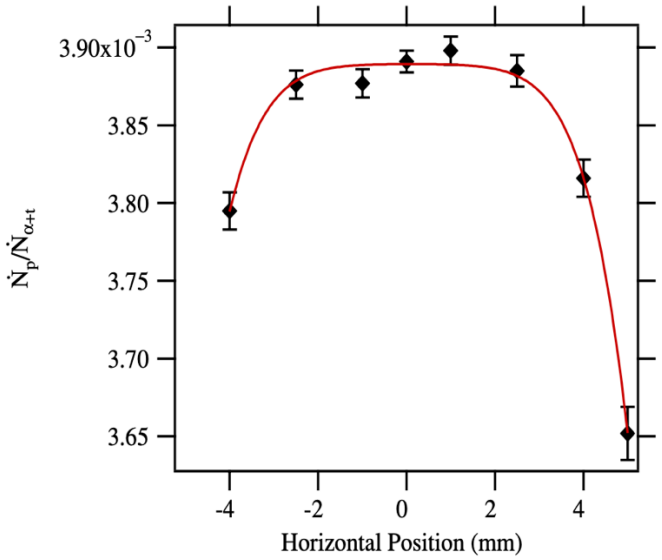

Figure 3. 2 Proton rate as a function of the detector's horizontal position normalized to the neutron detector counting rate. A fit to the data points is shown by the solid line [10].

3.1.1.5 Counting Neutrons

One may determine the precise number of neutrons that entered the proton trap by counting the products of the ^{6}Li (n, t)^{4}He reaction and comparing those rates to the input neutron fluence rate. The neutron fluence rate, total detector solid angle, neutron absorption cross-section, and

deposit areal density all affect how quickly these reaction products may be identified. Four silicon semiconductor detectors with solid angles created by properly machined apertures surround the target in the detector, which comprises silicon semiconductor detectors, and it counts the tritons and alpha particles created by neutron capture on the 6Li. It is shown schematically in the figure 1.1. The selected geometry is such that the first order in the source location does not affect the solid angle subtended by the alpha detectors. There are two of these devices; efforts have been made to measure absolute neutron fluence at the 0.1% level with the second one.

The target in the neutron monitor is a thin silicon wafer with a diameter of 50 mm and a layer of evaporated 6LiF. It has a thickness of around 0.4 mm. This thin deposit does not significantly alter the neutron fluence rate, and the 6Li (n, t)4He reaction products pass through it with little scattering or energy loss. To identify the alpha particles and tritons produced by the neutron absorption processes in 6Li, four surface barrier detectors are employed. These detectors have solid angles and precision diamond-turned apertures around them. The Figure below displays a typical pulse-height spectrum from one of the silicon detectors [10]. The electronic noise can be easily separated from the triton and particle peaks.

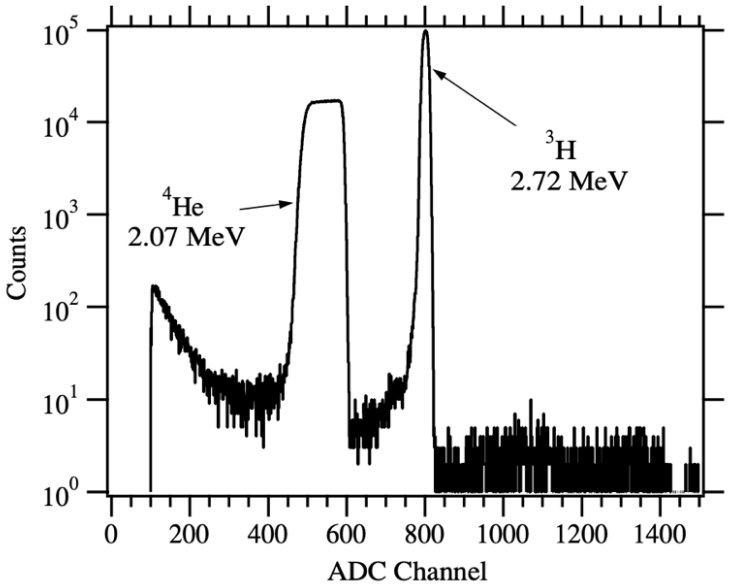

Figure 3. 3 An example of a typical pulse-height spectrum from 6 Li reaction products impacting a silicon detector in the neutron monitor [10].

3.2 Nab Experiment on Neutron Beta Decay

BL3 will use a similar detector as Nab. To properly estimate estimations of electron energy and proton momentum from proton flight periods, nab employs a novel long asymmetric spectrometer that distributes decaying electrons and protons onto two large-area silicon detectors. The Fundamental Neutron Physics Beamline of Oak Ridge National Laboratory's Spallation Neutron Source is where the Nab spectrometer is in use. The beta decay of unpolarized neutrons is connected to the Nab experiment. The electrodes, detection system, electronics, and electric and magnetic field profiles are all shown in detail by Nab spectrometers [16].

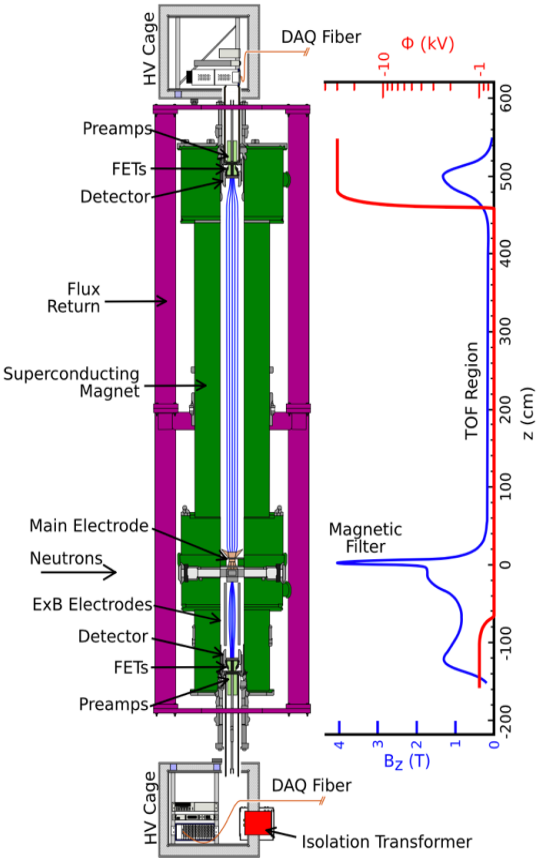

Figure 3. 4 A detailed illustration of the Nab spectrometer [16].

The electron-neutrino correlation parameter in neutron beta decay is measured by the Nab experiment with a relative accuracy of the order of 10^{-3}. This result allows independent and accurate determination of $\lambda = g_A / g_V$. When neutron lifetimes are measured with an uncertainty

of < 0.3 s, the expected Nab value λ provides competitive accuracy in determining Vud and nuclear super-permissive 0+ → 0+ decays in the CKM homogeneity check. Initial magnetic field tests show that the results are as expected. Precise measurements of the field and Installation of additional beamline components are commenced, and simulation research on systematics remains a continuing intensive work.

The detector developed for Nab is unique because it is designed to directly detect recoiling protons and electrons with excellent energy, time resolution, and position sensitivity. It is 1.5–2 mm thick and has a silicon detector with an active area of 100 cm^2 divided into 127 hexagonal pixels. This detector was created in association with the UCNB and Micron Semiconductor, Ltd. With an entry window (dead layer) of 100 nm and an energy resolution of 3 keV measured using a proton beam at the Triangle University Nuclear Laboratory, the detector surpasses the criteria of this Nab experiment. It has been possible to find protons with energy as low as 15 keV. Proton detection at Nab takes place at a -30 kV accelerating potential.

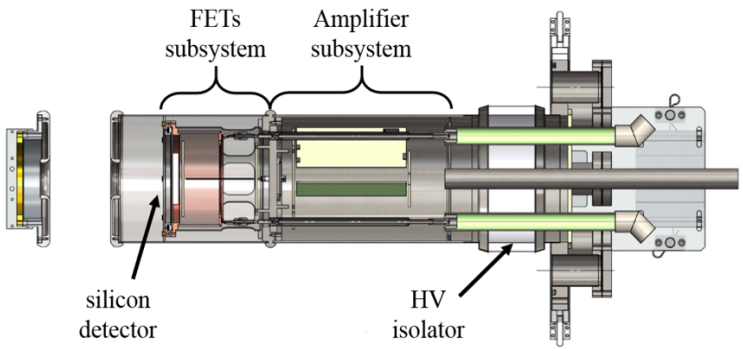

Figure 3. 5 A picture of the prototype detector mounting assembly [17].

To assess the predicted performance, a prototype detecting system has been created. The prototype has 18 pixels aggregated into 4 channels of 4 or 5 pixels and 19 measured single pixels. Two subsystems make up the preamplifier. The first one has three boards with eight channels each, FETs, and feedback loops. It is hooked to a detector in a vacuum and is linked to a liquid nitrogen line, connected to a cooler to install in room temperature air. To attach the detectors at 0.6 T in the region of field expansion and insert them into the UCNA spectrometer, a mounting

mechanism was developed. The design characteristics of the UCNA spectrometer, especially regarding the diameter, are comparable to those of Nab. The mount incorporates a 30 kV ceramic high voltage isolator that allows the data collection system, electronics, and detector to be exposed to a -30 kV accelerating potential.

3.3 Bottle and Beam Lifetime Experiment Variations

The current worldwide average lifetime measured by the bottle and beam method is τ_{bottle} = 879.4 ± 0.6 s and τ_{beam} = 888.0 ± 2.0 s [13]. The difference between these values is > 4σ, therefore, highly unlike that, the distinction is related only to statistical variability. To further comprehend this discrepancy, it is crucial to identify weaknesses in the two test methodologies.

Another reason why there might be a difference between τ_{bottle} and τ_{beam} is the existence of an important decay channel that is distinct from the classical β decay. The bottle experiment is sensitive to each neutron decay channel because it counts the number of neutrons that remain stable. In contradiction to this, Beam experiments count the free protons that are produced as neutrons decay; therefore, they are not sensitive to neutron decay pathways that do not yield free protons.

3.4 Simulation Tools

The BL3 collaboration uses different simulation tools to check the beam method's effects, including Greant4, SRIM, and PySRIM.

3.4.1 GEANT4

The high-energy physics community is working on GEANT4, a more comprehensive framework, to deal with the movement of energetic particles in matter. GEANT4 is generally a subatomic physics-friendly program. We use it for pre-subatomic physics experiments. To create statistical distributions of particles as they travel through various forms of materials, GEANT4 is used. In comparison to SRIM, the GEANT4 collaboration has created a far bigger toolset to handle

extremely complicated geometries and incorporates many more physical processes than only conventional electrical and nuclear stopping into their calculations. Nuclear reactions, particle showers, and other effects are crucial for modelling the complete system for many contemporary concerns, such as the physical behaviour of semiconductor devices in space settings. A group of physics constructors are used to create GEANT4 physics lists. A certain subset of particles and physics processes are implemented by each physics function. One of the three required user classes for the GEANT4 toolkit is the Physics List. Users can compare results obtained in the same conditions in different setups. Examples include SNR, SSS, EM, EMopt1, Livermore, EM low energy, EM WVI, elastic, binary etc. GEANT4 includes all essential physics processes for long and short-lived particles with energies ranging from tens of eV to TeV scale, including electromagnetic, hadronic, decay, and optical processes. To fill the gap between SRIM's efficient handling of low-energy processes in simple geometries and the extremely generic framework for nuclear events and complicated geometries already included in GEANT4.

Being object-oriented reduces the complexity of changes and modifications in existing simulations. For example, replacing one physics model with another has no effect rest of the simulation. In addition, multiple models of different energies can be combined in one simulation. Additionally, GEANT4 can be combined with other object-oriented tools such as ROOT.

3.4.1.1 Shapes and Materials in GEANT4

Several pre-programmed forms from GEANT4 can be combined to create volume hierarchies (more specifically, directed acyclic graphs of volumes). To efficiently browse geometry and embed volumes into other volumes, hierarchies are required. However, the automated "voxelization" procedure is chiefly responsible for efficiency. This procedure involves slicing space in its third dimension, resulting in each slice having a negligibly small volume. As a result, it takes less time to compute where traces are in the geometric model.

The necessary classes that specify the geometry will be coded by the application builder. A "logical volume" that includes geometry, materials, visualization properties, etc. is a basic unit that may be labelled "sensitive" to trigger user code when particles pass through it. Materials are

classified according to their density and isotopic or elemental makeup. For high-energy interactions, elements with an average atomic weight are desirable, however, isotopes are advised, especially in low-energy nuclear processes.

There are numerous ways to arrange logical volumes. As a simple placement, you can specify the space and place it any number of times. Transformation concerning the parent volume. Divide the parent volume into uniform sections as a "duplicated arrangement", Length, radius, or angle (depending on basic shape). They are saving parameters in memory as a "parameterized arrangement" that may represent any number of volumes of the same kind, calculating parameters as needed to perform a placement. Placements inside placements are a possibility. Another name for placement is "physical volume."

3.4.1.2 Advanced Characteristics

GEANT4, short for "Geometry and Tracking 4," is an advanced software toolkit designed for the simulation of the passage of particles through matter. Developed by the CERN collaboration, GEANT4 serves as a powerful and versatile simulation framework in the field of high-energy physics, enabling researchers to model the interactions of particles with materials accurately.

This toolkit is particularly valuable in experimental setups, allowing scientists to simulate the behaviour of particles such as electrons, protons, and photons as they traverse complex geometries and interact with different materials. GEANT4 incorporates a wide range of physics processes, covering electromagnetic and hadronic interactions, as well as decay processes, ensuring a comprehensive representation of particle behaviour.

Key features of GEANT4 include its modular and extensible architecture, enabling users to customize simulations for specific experimental setups. It provides a detailed and realistic representation of detector geometries, materials, and particle interactions, making it an indispensable tool in the design, optimization, and analysis of experiments in high-energy physics, medical physics, space science, and other related fields.

GEANT4 has many other important features, but I will briefly mention them here. For example, they are subdividing, merging, and mirroring volume hierarchies—a tool for checking the overlap of geometry volumes. Semitransparent bodies can be used to connect to CAD systems. To facilitate impact evaluation, dosage distribution, etc., parallel (non-physical) geometry is used. events that are biased or weighted, as well as other methods for reducing variation. a flexible command structure that enables interactive parameter setting. Applications are frequently created using built-in and application-specific commands and are primarily programmed. A flexible visualization tool for looking at geometry, paths, and hits. interface for Python. Simple forms are combined, intersected, and subtracted using Boolean operations.

3.4.1.3 GEANT4, A Monte Carlo Simulation Toolkit

In many domains and phases of experimental physics programmes, simulations are essential. Design of the experimental apparatus, assessment and identification of the project's possible physical results, assessment of the project's potential dangers, and assessment of the experimental performance; helping with calculation and verification of the object-oriented toolkit from GEANT4 is a comprehensive collection of C++ libraries that let users simulate their detector systems. The software system autonomously transfers the shot particles to the detector based on the detector's shape, simulating the interaction of the particles with the material using Monte Carlo techniques. One such approach is solving arithmetic problems using statistical sampling and random numbers.

GEANT4 was primarily created to simulate next-generation HEP detectors (ATLAS, Alice, CMS, LHCb, etc.), but it is now extensively used to simulate detectors of the present generation as well as in the fields of space and medical physics. If the necessary interaction processes have been incorporated into the toolkit, any experimental system based on particle interactions might theoretically be reproduced in GEANT4.

3.4.1.4 Neutron Interactions in Geant 4

The neutron interaction is split into four distinct parts, treated as elastic scattering, and the final state is obtained by scanning the differential cross-section. Radiation trapping is given by photons whose final state is generated. Inelastic scattering of different final states is now supported. Different models are available for each of these processes, provided as several predefined physics lists for specific applications such as medical applications and low background physics.

There are some issues with the way GEANT4 handles inelastic scattering. At the state level, recoil is handled correctly, but on an event-by-event basis, momentum and energy conservation are violated. In the inelastic process of GEANT4, neutrons and bouncing nuclei form composite particles that isotopically decay back to neutrons within the nucleus. However, inelastic scattering can be implemented with different physics lists in many ways. Therefore, testing the fundamental reactions between neutrons and nuclei in GEANT4 physical processes is necessary.

3.4.1.5 Screened Nuclear Recoil in GEANT4

Screened nuclear recoil was introduced as a process in GEANT4 which is used to describe backscattering, forward scattering, and energy deposition in silicon. It is a procedure that modifies nuclei-to-nucleus screened coulomb collision. A single scattering process replaces many scattering processes for protons and ions. A statistical distribution of the particles is created using it. The screening keys, also known as the screening functions, are used to filter nuclear recoil. The standard functions are "zbl" (recommended for soft scattering), "lj" (recommended for backscattering) and "mol" (Moliere potential). In materials research and computational physics, the Ziegler-Biersack-Littmark (ZBL) potential is a commonly utilized scientific interatomic potential. It is mostly used to simulate atom-to-atom interactions in molecular dynamics simulations of different materials, especially metals. GEANT4 was significantly limited when the Ziegler-Biersack-Littmark (ZBL) universal scattering technique was included [7]. The ZBL potential is named after the scientists who developed it: James F. Ziegler, Joachim Biersack, and Ulf Littmark, who introduced it in their paper published in 1985. In GEANT4, the Moliere potential is utilized as a parameterization of multiple scattering for simulating the interactions of high-energy

particles with matter. This potential is particularly employed in the simulation of electromagnetic interactions, such as electron and positron scattering, in materials. The Lennard-Jones potential is commonly referred to as "lj" in GEANT4. A common mathematical model for explaining the interaction between two neutral atoms or molecules is the Lennard-Jones potential. It is frequently used in Monte Carlo and molecular dynamics simulations to simulate the interactions between atoms or molecules in a material. The class's public procedures, which are given below, directly assist the user in setting the physical parameters [14].

3.4.1.5.1 Method

The user may define numerous significant physical parameters in the function for this operation.

1. The screening function requested by the external Python module that creates the screening table and cross-section is chosen by the screening key.

2. Controlling Generate Recoils determines whether local energy buildup takes place with an energy that would have otherwise been passed to the recoil particles, as opposed to recoil particles being formed and monitored.

3. RecoilCutoff determines the energy below which entering particles cease without further interaction and below which there is no recoil. If given the chance, stopped particles can build up energy and degrade ("stop and live" if the stopping process is present, otherwise "stop and kill").

4. Physics The energy cut-off utilized in the above calculation of the total scattering cross section is chosen by the cut-off. For issues where forward multiple scattering is crucial, its value is typically fixed between 1 eV and 10 eV. To maximize efficiency if backscattering is an issue, it can be raised to 100 eV or higher. The mean free path will vary when this parameter is changed, but the change won't be noticeable till the mean free path approaches the length scale of the substance the particles are moving through.

3.4.2 SRIM (Stopping and Range of Ions in Matter)

SRIM, which stands for Stopping and Range of Ions in Matter, is a widely used computer software package designed for simulating the interactions of energetic ions with matter. Developed by the National Nuclear Data Center (NNDC) at the Oak Ridge National Laboratory, SRIM is particularly utilized in the field of ion-beam physics and materials science.

The primary purpose of SRIM is to calculate the stopping power, range, and other related parameters of ions as they traverse through various materials. The software employs a combination of theoretical models and experimental data to simulate the behaviour of ions, considering processes such as electronic and nuclear stopping, energy straggling, and range straggling.

Researchers and engineers often use SRIM to predict the penetration depth of ions into materials, assess the effects of ion irradiation on target materials, and optimize experimental parameters for ion-beam applications. The software is valuable in diverse areas, including semiconductor device manufacturing, ion implantation, radiation damage studies, and ion-beam analysis.

A point-like monoenergetic input beam is used in a typical SRIM Monte Carlo simulation. It is a collection of particles (history) that disregards the incident beam's true ion-optical characteristics. The incident beam's ion optical properties are used by the beam-generating module to create a TRIM.DAT file. In an interactive window, the user specifies these options. A typical SRIM simulation and a realistic beam simulation are shown side-by-side in the illustration below. There is also a beam emission diagram provided by the module. There may be some area distribution throughout the beam spot because of the incident beamline's possible coloration [15].

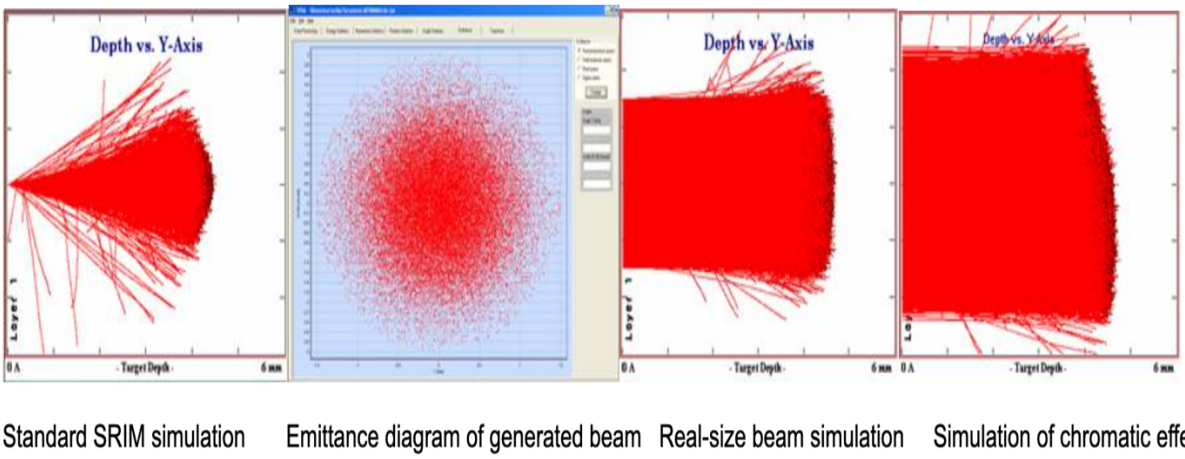

Figure 3. 4 A typical SRIM simulation is compared to a real beam simulation [15].

A group of software programs called SRIM calculates a variety of ion transport in material characteristics. The following examples are typical applications.

3.4.2.1 Ion Stopping and Range in Targets

With SRIM, which measures the stop and extent of ions in matter, most of the energy loss of ions in the matter is measured. For each ion at any energy and any elemental target, SRIM provides quick computations that yield tables of stopping power, range, and scattering distributions. Targets with intricate multilayer structures are used in more sophisticated computations.

3.4.2.2 Ion Implantation

By implanting atoms into samples, ion beams can change the target's chemical and electrical characteristics. Atomic displacement damage is another effect of ion beams on fixed objects. The SRIM package contains most of the kinetic consequences of these kinds of interactions that are physics-related.

3.4.2.3 Sputtering

In an ion-sputtering process, an ion beam can destroy target atoms. Calculations for sputtering by any ions at any energies are included in the SRIM package.

3.4.2.4 Ion Transmission

When using energy-absorbing blocks to lower the energy of the ion beam or in ionization chambers, the ion beam can be tracked through a mixed gas/solid target layer.

3.4.2.5 Ion Beam Therapy

Ion beams are widely used in radiation oncology and scientific treatment. There are common programmes provided.

The SRIM interface is quite like doing a SRIM computation, a list of layers forms is included in the idea. A Layer is a list of elements with density and width. An element's name, atomic number, symbol, and custom mass [amu] can all be given. Ions are like elements except that they also need energy measured in [eV].

3.4.3 PySRIM

PySRIM refers to a Python interface or wrapper for SRIM (Stopping and Range of Ions in Matter). This Python package allows users to interact with SRIM functionality using Python programming language.

The development of PySRIM is aimed at providing a more user-friendly and flexible interface for those who prefer using Python for their scientific computations and simulations. It allows researchers and scientists to incorporate SRIM simulations into their Python-based workflows, making it easier to analyze and visualize results.

Users can use PySRIM to perform tasks such as calculating ion ranges, energy deposition profiles, and other relevant parameters within the Python environment. It simplifies the process of setting up SRIM simulations and extracting data for further analysis.

TRIM keeps all cascades in memory, it is prone to crashes. Large runs with entire cascades of more than 1,000 ions will therefore exhaust the available memory. PySRIM provides an easy-to-use input file API wrapper that runs on all OS systems and overcomes all these problems.

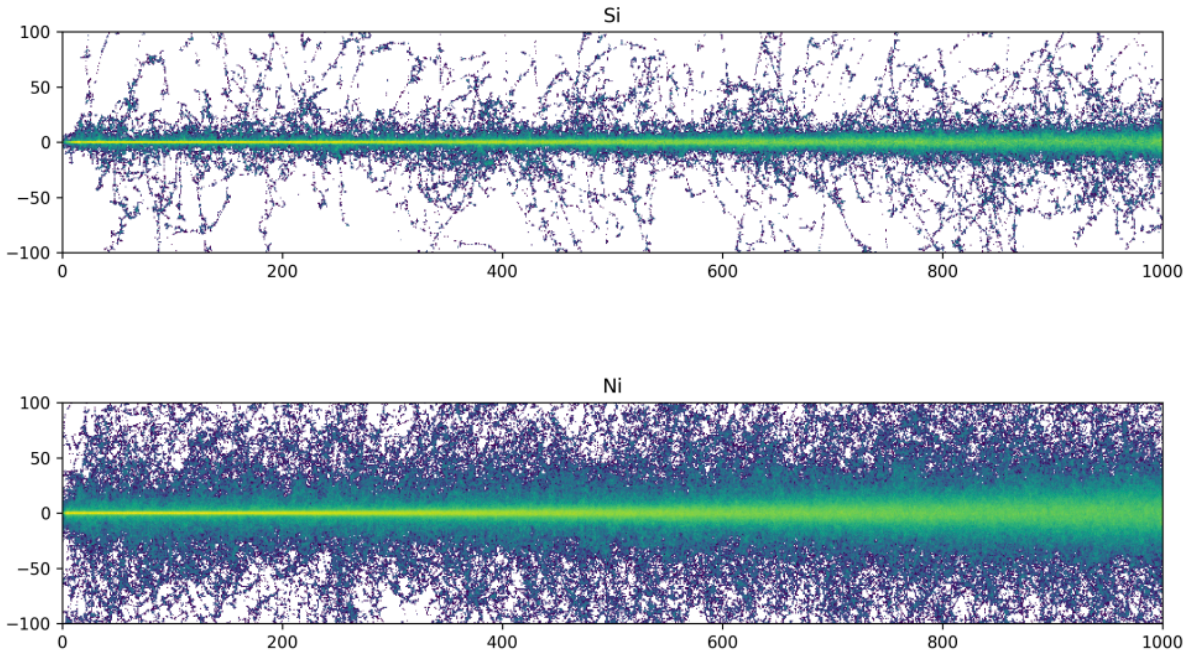

Figure 3. 5 Diagram of ion vacancies moving through SiC created by PySRIM. (Upper) 21 MeV Si Ion (bottom) 21 MeV Ni ion [15].

3.4.3.1 Characteristics of PySRIM

Python Interface: PySRIM serves as a Python wrapper for SRIM, allowing users to leverage the functionality of SRIM within a Python environment.

Ease of Use: The main goal of PySRIM is to make it easier for users to perform SRIM simulations and analyses using Python. This includes setting up simulations, running them, and extracting relevant data.

Integration with Scientific Computing Ecosystem: Being a Python module, PySRIM integrates well with other scientific computing libraries and tools in the Python ecosystem, such as NumPy and Matplotlib.

Customization: PySRIM may provide users with the flexibility to customize simulations and analyses according to their specific needs, building on the capabilities of SRIM.

Data Analysis: The module likely includes functions to analyze the results obtained from SRIM simulations, making it easier for users to interpret and visualize the data.
Documentation: Like many open-source projects, PySRIM likely comes with documentation that guides users on installation, usage, and advanced features.

The text files IONIZ.txt, VACANCY.txt, NOVAC.txt, E2RECOIL.txt, PHONON.txt, RANGE.txt, and COLLISON.txt are resolved by PySRIM. The COLLISON.txt file can get rather large; hence the Collision parser uses a buffered reader that can handle any file size. Moreover, there is a class named SRIM. output. A dictionary of each processed output file is returned as part of the results, which evaluate all output files in a directory. PySRIM comes with various charting options, such as the ability to plot the DPA against depth. The most powerful aspect of PySRIM is that all text files are accessible as NumPy arrays.

3.5 Various Experiments on Neutron Lifetime

3.5.1 Beam Neutron Lifetime Experiment by NIST

At various times over the last 60 years, experimental results on neutron lifetimes have agreed or disagreed. Notably, the value from the most accurate beam experiment conducted at the NIST Center for Neutron Research is 8.9 seconds (standard deviation 3.9) higher than the average UCN storage value using materials and magnetic bottles. Other beam method results are similarly high but with greater uncertainty. This discrepancy has been widely discussed in both the scientific literature and popular media in recent years. NIST experiments play an important role here. This is because it has been reported to have higher accuracy compared to other beam measurements. The below figure [18] shows a fitting curve where the detector backscattering percentage is shown against the observed neutron lifetime. The free neutron lifetime is extrapolated to zero backscattering.

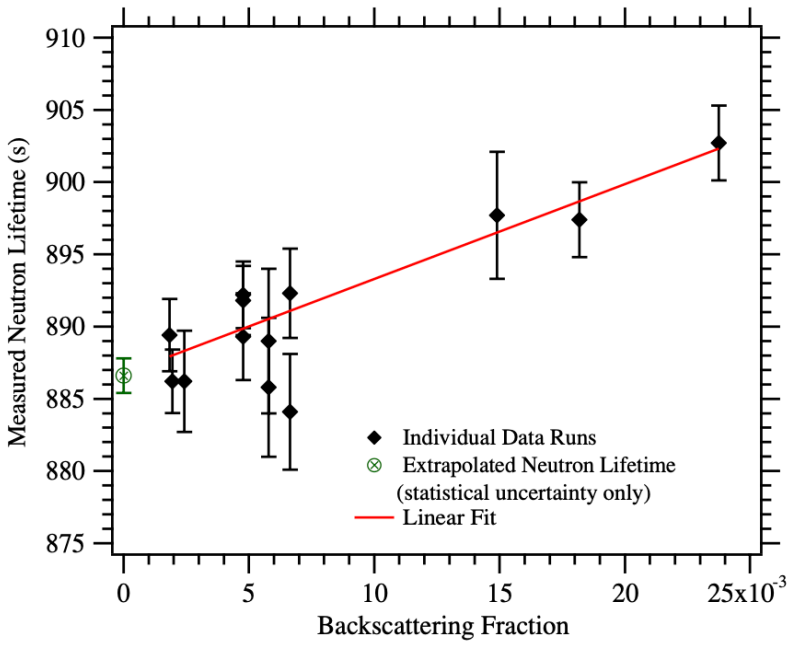

Figure 3. 6 A linear fit of the measured neutron lifetime versus the detector backscattering fraction. The extrapolation to zero backscattering gives the free neutron lifetime [18].

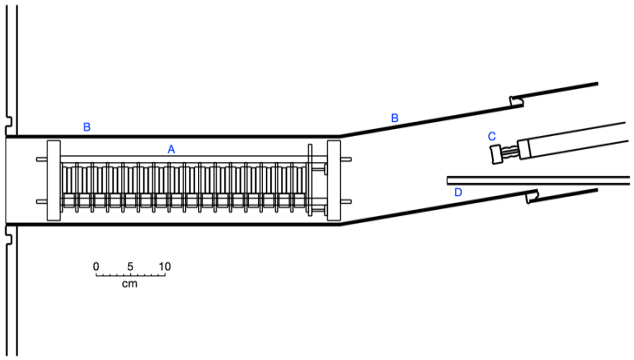

Figure 3. 7 Arrangement of the proton trap apparatus in the NIST beam neutron lifetime experiment. A) proton trap; B) 8 K magnet bore; C) silicon proton detector; D) quartz neutron guide [18].

A large class of potential systematic effects in beam lifetime experiments, including residual gas interactions, cause loss of protons from traps on the millisecond time scale. On a millisecond time scale, the loss of protons from traps is caused by a broad class of possible systematic effects in beam lifetime experiments, including residual gas interactions. Repeated neutron lifetime measurements with acquisition durations ranging from 1 ms to 100 ms will be used to identify these effects. The trap becomes unstable for durations longer than 10 ms, therefore this was not

possible in this original NIST test. Such a measuring programme is the focus of the current BL2 effort and a key objective of upcoming BL3 investigations because of the increased trap stability.

3.5.2 UCNτ EXPERIMENT

The UCN experiment uses ultracold neutrons (UCNs) in a magneto-gravity trap to precisely estimate the lifetimes of neutron beta decay. Neutrons are vulnerable to several additional loss processes because of their lengthy beta-decay lifetimes, including up scattering, absorption at material surfaces, and spin flipping. Precision experimental observations may be particularly challenging because these interactions may work on timeframes close to neutron beta decay. The objective of this experiment is to decrease the measurement uncertainty of neutron lifetimes longer than one second.

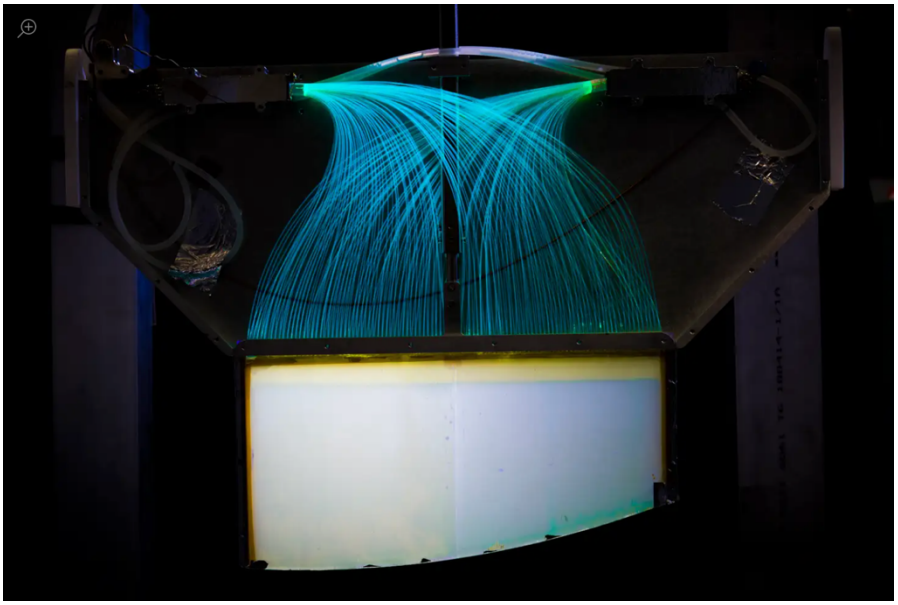

Figure 3. 8 The Neutron Science Center's primary detector for neutron counting during the UCNτ experiment [19].

The investigation of neutron decay is evolving into a strong theoretical and experimental test of the standard model with increasing accuracy. The existence of new physics leading to proton-less neutron decay channels in the final state or the existence of systematic effects of underestimated or unidentified ones is shown as one of the tricks in the current puzzle resulting from discrepancies between "beam" and "bottle" methods of τ_n measurement. Dark matter particles

produced by neutron decay might be the cause of the former. Measurements of τ_n with an error of 0.34 s (0.039%) [20] utilizing two blinded data sets from 2017 and 2018. These measurements outperform earlier findings by a factor of 2.25. Improved experimental and analytical methods are part of the new findings.

Figure 3. 9 The image shows the Los Alamos National Laboratory's UCNtau experiment measuring the neutron lifespan using the "bottle technique" [20].

The finding was consistent throughout all lifetime measurement runs:

- Spallation neutrons generated by an 800 MeV proton beam collision with a W target are the first step in creating UCN. The gate valve opens concurrently, enabling UCN to diffuse from the source to the trap. Through a hole at the bottom of the trap, UCN enters. The cleaner and primary detector are lowered to cleaning height once the trap is loaded with UCN.

- UCN generation comes to an end as soon as the gate valve and the aperture at the bottom of the trap close. The cleaner is left at cleaning height for a considerable amount of time while the primary detector is elevated to the top of the trap.
- UCNs are confined in traps at intervals ranging from 20 to 5000 seconds.
- The primary detector is lowered to count the remaining UCNs in the trap.

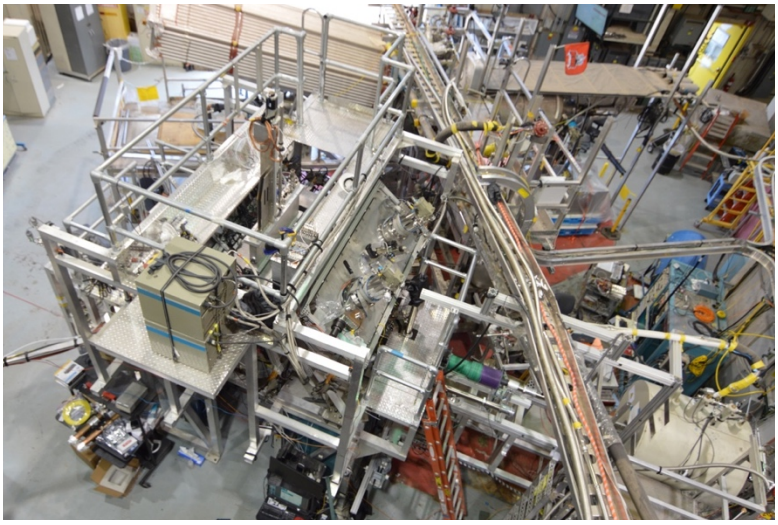

Figure 3. 10 UCN Magneto-gravitational trap.

UCNτ device configuration for the 2018 campaign [19] shows the UCN, cleaning surface, principal detector, and monitor take up the most space. For UCN, a polarising magnet chooses a strong magnetic field. The UCN is then placed into the trap after being "pre-cleaned" in a buffer volume and rotated into a trappable low-field search spin state.

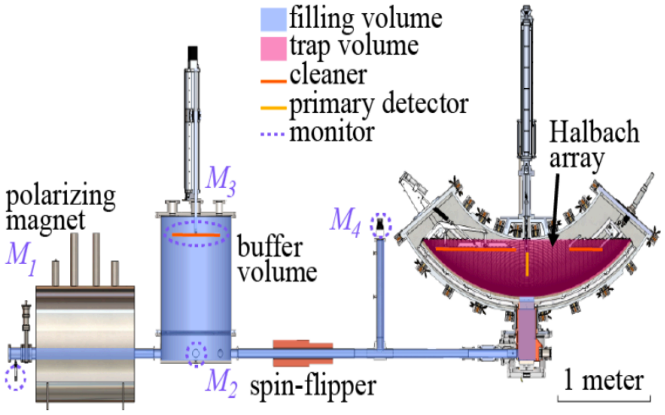

Figure 3. 11 The Experiment Apparatus of UCNτ [21].

3.5.3 NASA Lunar Prospector and Lifetime of a Neutron

For the τn base, there are currently two opposing values about the outcomes of two various types of laboratory test trials. In "bottle" experiments, the number of neutrons released from the material in magnetic, gravitational, or real traps is counted over time. This production rate of β-decay products in neutron rays that pass through the capture zone is measured in the "beam" experiment. Average beam measurements are off by about 4σ from the more accurate cryogenic trap neutrons. This contradiction has existed for 15 years of his life and has become known as the "neutron lifetime puzzle". Utilizing the information gathered by NASA's MESSENGER spacecraft during a Venus-Mercury encounter, a third method to determine τ_n from space has just been shown to be achievable. The fact that the planet's surface is continually blasted allows for the possibility of measurements of τ_n from space.

When galactic cosmic rays (GCRs) strike atomic nuclei, a significant number of high-energy neutrons are released. These neutrons' energy is reduced in successive collisions with surface area nuclei. Some neutrons collide with enough solid objects or the environment frequently enough to attain thermal equilibrium. These thermal neutrons often travel at speeds of many km/s. As a result, the flight distance across hundreds to thousands of kilometres between release and spacecraft detection is of the order of τ_n. The primary objective of planetary missions is to

measure the surface composition of 10 planets, Consequently, in such missions, several neutron spectrometers are used to learn more about planetary surface composition.

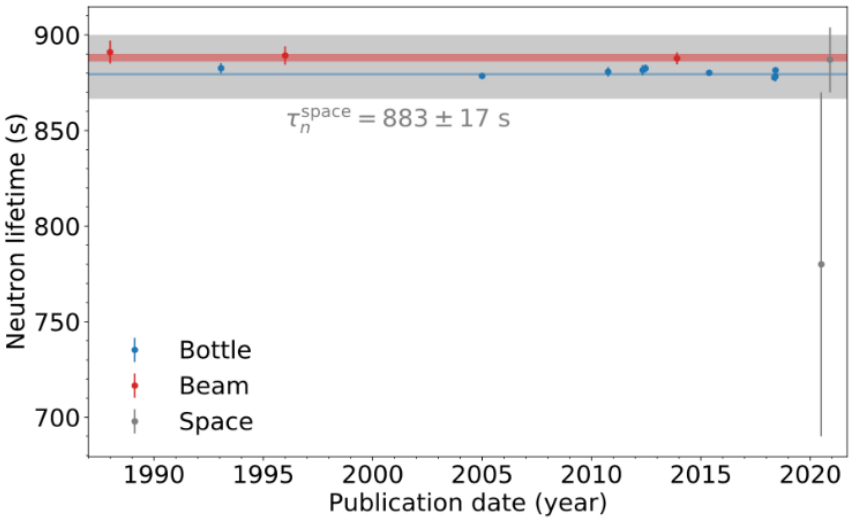

Figure 3. 12 Other recent measurements of the particle data group and τ_n the shaded areas represent the uncertainty-weighted standard errors of the mean lifetimes for each measurement class [22].

Chapter 4

Energy Deposition for Beam Lifetime 3 Experiment

In this chapter, the BL3 simulation using SRIM and GEANT4 is explained. The energy deposition and backscattering/transmission of 35 keV protons on a silicon detector are investigated using the example in TestEm7/StandardNR, G4BL3/SNR, and the physics list in GEANT4. Additionally, we contrast the results with SRIM and verify the energy buildup in GEANT4's various processes and its impact on the ratio of different components.

The development of the Beam Lifetime 3 experiment is ongoing. It will use a new, considerably larger magnet and trap to handle a bigger neutron beam and a greater proton counting rate. It will make use of a segmented large-area proton detector. Different systematic advancements in proton counting, a decrease in proton backscatter, and magnet trap uniformity are predicted with a final uncertainty aim of 0.1 seconds in neutron lifetime.

4.1 Proton Interaction in Silicon

Proton interaction in silicon with energy 35KeV was studied using GEANT4 and the result is shown below:

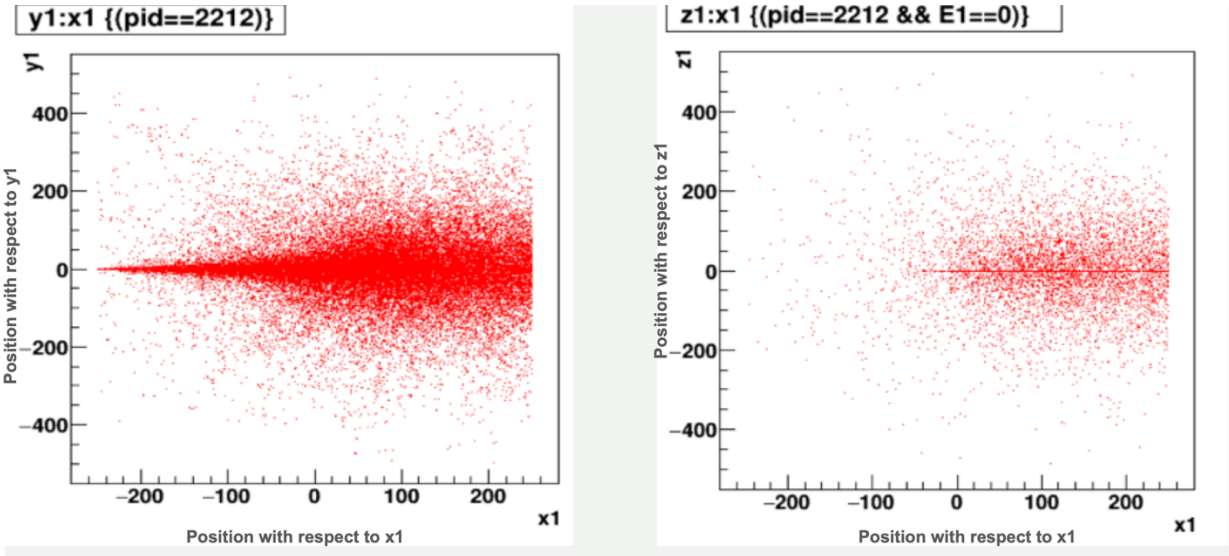

Figure 4. 1 Proton Interaction in silicon with energy 35KeV.

By contrasting the screen nuclear recoil and single scattering models employing 35 KeV energy, the comparison of the final proton location is examined. Calculations of the longitudinal and radial ranges as well as research into the backscattered and transmitted proton fractions are made. The comparison of the final proton position is described in the table below:

Table 2 Comparison of the final proton position.

35KeV Proton on Silicon	**GEANT4 TestEm7 SNR**	**GEANT4 TestEm7 SSS**
Longitudinal range: mean	416.001 nm	405.101 nm
Longitudinal range: straggle	110.706 nm (RMS)	74.7656 nm
Radial range: mean	92.2198 nm	119.929 nm
Radial range: straggle	94.2622 nm (RMS)	92.1669 nm
Fraction of backscattered	0.0538% +/- 0.02%	0.448% +/- 0.006%
Fraction of transmitted p's	15.244% +/- 0.012%	30.158% +/- 0.054%

The percentage of backscattered and transmitted components is also displayed in the image below, where we can see the standard and mean deviation and the total number of entries that were analyzed.

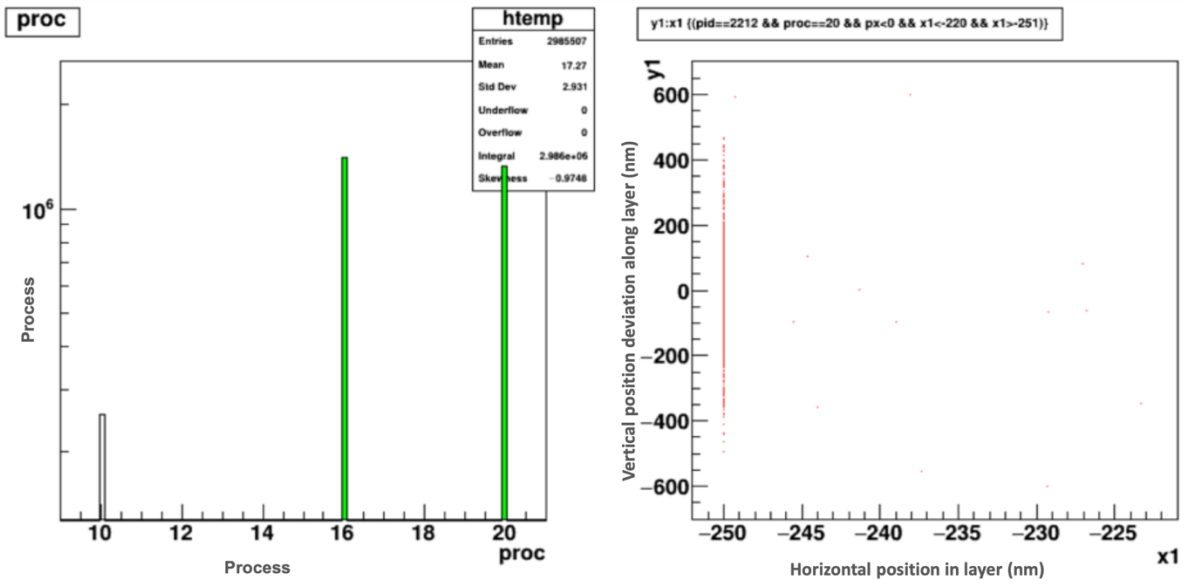

Figure 4. 2 Backscattered protons for a 35 keV proton beam on a silicon layer from -250 nm to 250 nm, as identified by a negative z-component of the momentum when a simulation step ends in the first 30 nm of the silicon.

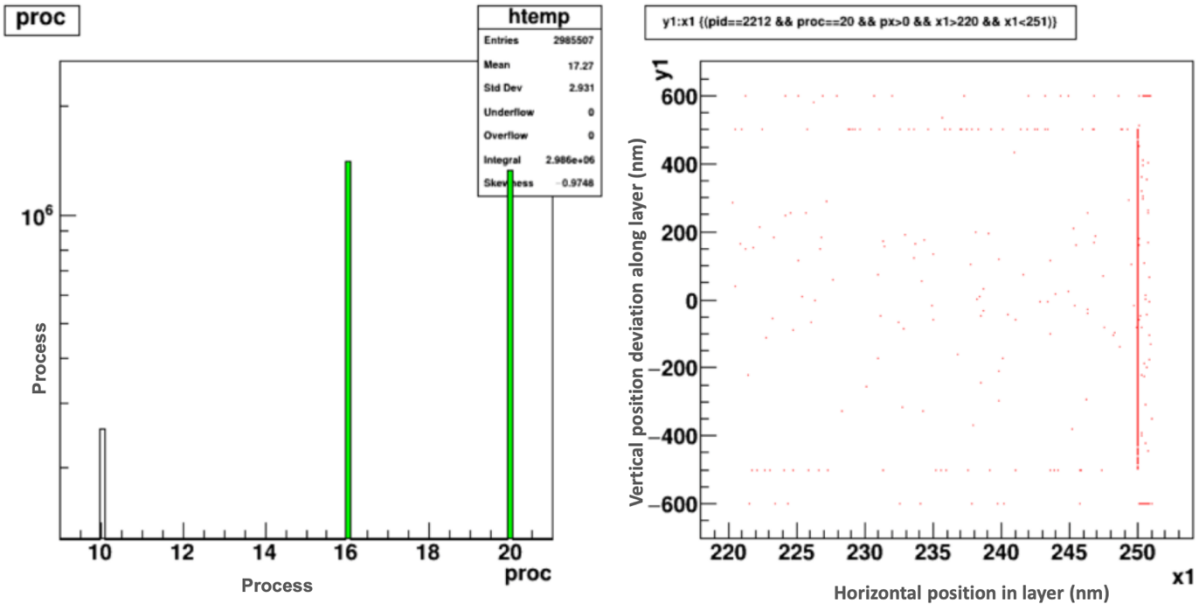

Figure 4. 3 Transmitted protons for a 35 keV proton beam on a silicon layer from -250 nm to 250 nm, as identified by a positive z-component of the momentum when a simulation step ends in the last 30 nm of the silicon.

The chart below shows how much protons are transmitted and how much is backscattered, illustrating the impact on the individual components.

Table 3 Fraction of specific components.

Components	Transmitted protons (100k events)	Backscattered protons
Standard NR	28818=28.81%=+/-0.169%	428=0.428%=+/-0.02%
Standard SS	0	260=0.26%=+/-0.016%
Empenelope	15295=15.29%=+/-0.12%	69=0.069%=+/-0.008%
Elastic	15197=15.19% =+/-0.12%	47=0.047%=+/-0.006%
Binary	15197=15.19%=+/-0.12%	47=0.047%=+/-0.006%
Binary ion	15335=15.33%=+/-0.12%	50=0.05%=+/-0.007%

EmStandard_opt0 EmStandard_opt1 EmStandard_opt2 EmStandard_opt3 EmStandard_opt4	15335=15.33%=+/-0.12% 15335=15.33%=+/-0.12% 15335=15.33%=+/-0.12% 15335=15.33%=+/-0.12% 15295=15.29%=+/-0.12%	50=0.05%=+/-0.007% 50=0.05%=+/-0.007% 50=0.05%=+/-0.007% 50=0.05%=+/-0.007% 69=0.069%=+/-0.008%
IonGasModels	15335=15.33%=+/-0.12%	50=0.05%=+/-0.007%
EmstandardGS	15335=15.33%=+/-0.12%	50=0.05%=+/-0.007%
EmStandardWVI	16=0.016%=+/-0.004% proc==26...2461	220=0.22%=+/-0.014%
Emlowenergy	14499=14.49%=+/-0.12%	69=0.069%=+/-0.008%
Emlivermore	15295=15.29%=+/-0.12%	69=0.069%=+/-0.008%

4.2 Energy of Proton

The amount of kinetic energy that a proton possesses because of its movement is known as its energy and is commonly expressed in electron volts (eV).

On the other side, a proton's energy deposition describes how much energy it transfers to a medium as it passes through it. The relationship between the energy of a proton and its energy deposition in a medium depends on several factors, including the proton's velocity, its charge, and the properties of the medium. Due to a proton's greater capacity to ionize and excite atoms and molecules in the medium, its energy deposition typically rises as a proton's energy does. Figure 4.4 illustrates the 35 keV energy of proton on silicon and provides information on the depth it reaches based on 10,000 events. Figure 4.5 shows 35KeV energy deposition of a proton on silicon with 10k events.

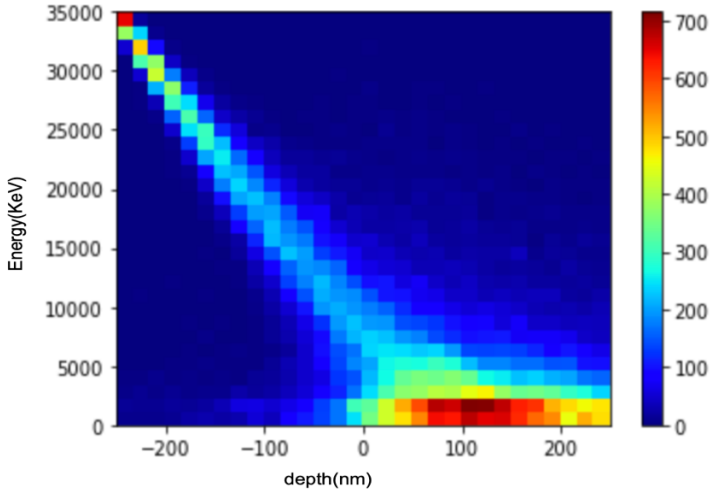

Figure 4. 4 An illustration of proton Energy.

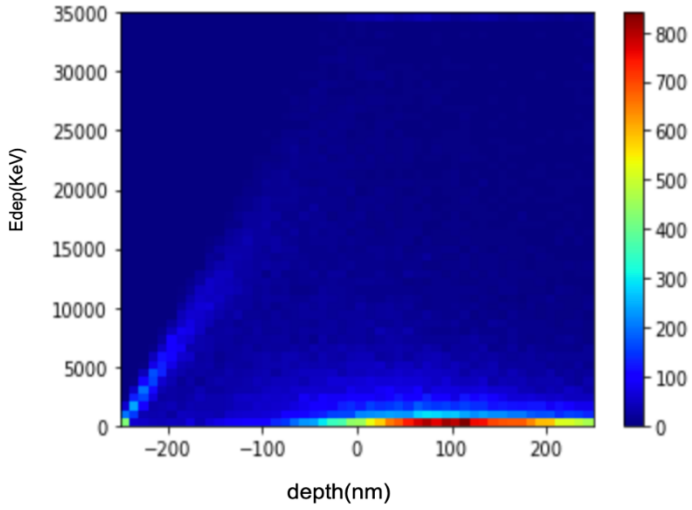

Figure 4. 5 An illustration of Energy deposition of Proton.

4.3 SNR Component

It is a method for handling screened nuclear Coulomb collisions. Different screening keys are implemented, such as zbl, mol, lj, and ljzbl. If the condition is true, ions hit by the primary are transformed into new moving particles in Generate Recoils. If the condition is false, energy is deposited but no new moving ions are produced. Even if Generate Recoils is true, there is a recoil cut-off energy below which no new moving particles will be produced. A fundamental particle will also come to a standstill if its energy drops below this threshold, and stop the energy transfer

that screening tables are calculated for in physics. There isn't a good reason to modify it from the usual 10.0 eV.

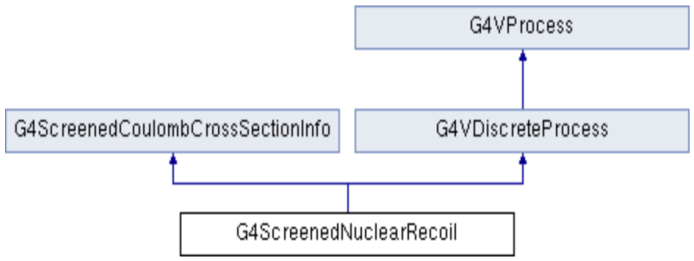

Figure 4. 6 A representation of G4ScreenedNuclearRecoil's inheritance.

The energy deposition by using Screen nuclear recoil is shown in Figure 4.7. The process that involves using the SNR model is also shown below. Physics Processes describe how particles interact with a material. In Figure 4.7 processes involved in the screen nuclear model are hIoni and transportation. The transportation process is responsible for propagating a particle through the geometry in an electromagnetic or gravitational field while hIoni is used as G4hIonisation.

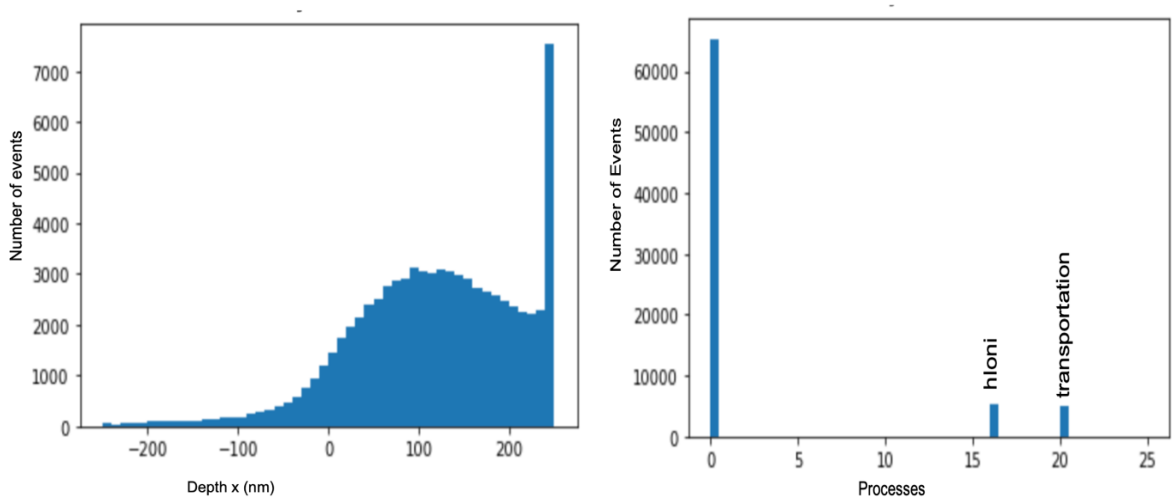

Figure 4. 7 The energy deposition for screened nuclear recoil with processes.

Processes are a family of models for physical interactions that include hadronic interactions as well as electromagnetic interactions involving leptons, photons, hadrons, and ions. All other operations are triggered by the category of tracking, which manages each process' contribution to the evolution of a track's state and provides information in delicate amounts for hits and digitalization.

4.4 Boron Implantation on Silicon

Boron implantation on silicon is a commonly used technique in semiconductor device fabrication. The process involves the introduction of boron ions into a silicon substrate, typically using ion implantation equipment. The purpose of boron implantation is to create regions of p-type conductivity in the silicon substrate, which are essential for the formation of p-n junctions in semiconductor devices such as diodes and transistors.

The boron ions are accelerated to high energies and then directed onto the surface of the silicon substrate. The ions' energy determines their penetration depth into the substrate, while the ion dose determines the concentration of boron in the substrate. The implantation process can be controlled to create regions of varying boron concentration and depth within the substrate.

After implantation, the boron ions are activated by annealing the substrate at high temperatures. This causes the boron atoms to diffuse and form a region of p-type conductivity in the silicon substrate. The resulting p-n junctions can then be used to create a variety of semiconductor devices. Boron implantation is a critical step in the fabrication of many types of semiconductor devices, and the precise control of implantation parameters is essential to ensure that the resulting devices meet their performance specifications.

A light bullet is fired at a heavy target during the implantation of boron into silicon to create high-angle scattering events. Boron is a dark, glossy semiconductor that is pure and crystalline. It conducts electricity like metal at high temperatures but turns into an insulator at low temperatures. Boron has a mass number of 11 and contains 5 protons and 6 neutrons. It has two

stable isotopes, B10 and B11. The exceptionally high thermal neutron capture cross-section (3,836 bar) of the boron-10 isotope makes it special (i.e., it readily absorbs low-energy neutrons). An alpha particle is eliminated when the nucleus of this isotope successfully absorbs a neutron.

Using one of Mendenhall's research findings [7], boron Implantation in silicon is used to demonstrate the effects of proton Implantation on silicon. Taking one of the results from Mendenhall's study, boron was implanted into silicon to show proton implantation on silicon [7]. The range of boron and its stragglers in silicon are shown in Figure 4.8. The implant profile is extremely narrow at high energies when most of the energy is lost to electrons, and the dispersion is low.

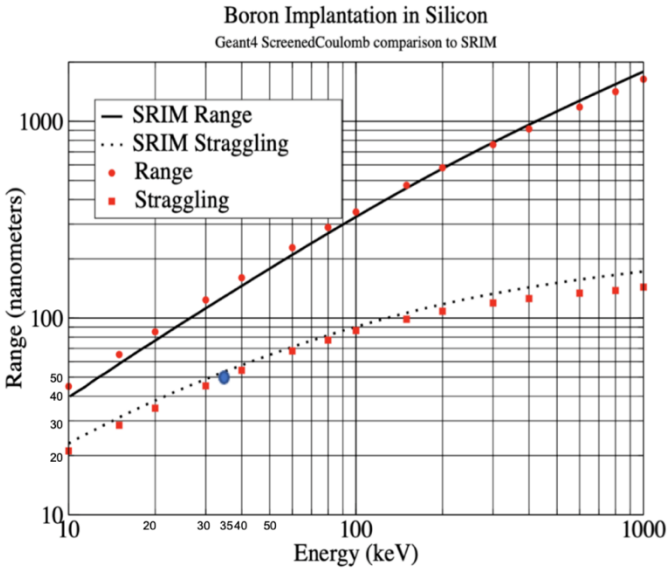

Figure 4. 8 Boron Implantation on Silicon [7].

In this simulation 35, keV boron on silicon was taken using GEANT4 screened nuclear recoil to verify the results and calculation was done on the vertical and radial ranges as well as the drag to prove the results. The below table shows the results of the data taken. The table shows that the lines where they intersect in the figure above are almost at the same position as they show boron implant results in the dotted line. Therefore, the calculations in these simulations are consistent with the results.

Table 4 Ranges of Boron using GEANT4 SNR

(35 KeV Boron on Silicon)	**GEANT4 TestEm7 SNR**
Long. range: mean	142.017 nm
Long. range: straggle	50.9224 nm (RMS)
Radial range: mean	48.016 nm
Radial range: straggle	36.327 nm (RMS)
Total Energy deposit	34.9406 keV
Niel energy deposit	10.221 keV

4.5 Proton Scattering in Silicon

The term "nucleons" refers to the combination of protons and neutrons, each of which has a mass of around one atomic mass unit. Although the proton was once thought of as an elementary particle, it is now characterized as a composite particle in the current standard model of particle physics because it contains three valence quarks and is now classified with the neutron as a sort of hadron. Protons are made up of two up quarks and one down quark. I have taken 35 KeV protons on silicon using GEANT4-screened nuclear recoil. I calculated the vertical and radial ranges. Figure 4.10 shows proton scattering in Silicon at different energy levels.

Table 5 Ranges of Proton in GEANT4 using SNR.

(35 KeV Proton on Silicon)	**GEANT4 TestEm7 SNR**
Long. range: mean	412.673 nm
Long. range: straggle	109.523 nm (RMS)
Radial range: mean	102.07 nm
Radial range: straggle	90.7 nm (RMS)

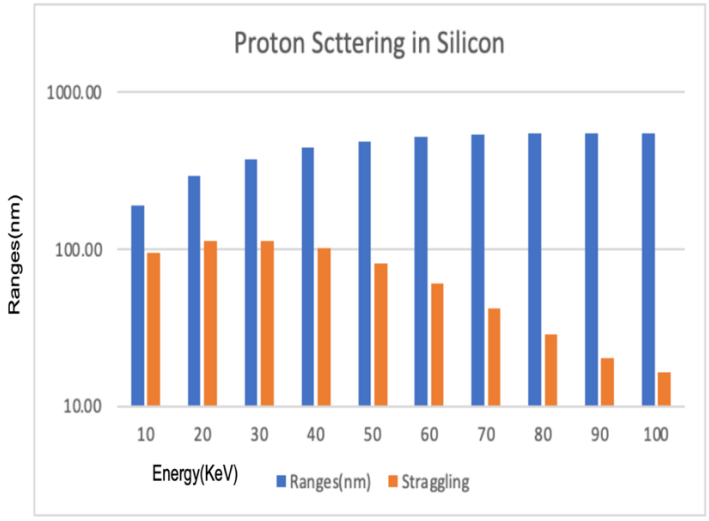

Figure 4. 9 Proton Scattering in Silicon.

4.6 GEANT4 Comparison to SRIM (50um Si) with Boron Implantation in Silicon

GEANT4 offers capabilities for managing user interface, visualization, tracking, detector response, runs, and geometry. On the GEANT4 platform, the Monte Carlo methods are utilized to "simulate the movement of particles through matter." It is the successor of the GEANT series of software toolkits developed by the GEANT4 cooperation and the first to use object-oriented programming (in C++). The international GEANT4 Collaboration oversees its development, maintenance, and customer support.

SRIM is a group of software programs that calculates a variety of aspects of ion transport in matter. SRIM quickly computes tables of stopping powers, range, and straggling distributions for each ion at any energy in any elemental target. More complex computations can employ targets with complex multi-layer structures. Ion Stopping and Range in Targets are frequent applications: Most of the energy loss of ions in the matter is calculated using SRIM, the Stopping and Range of Ions in Matter.

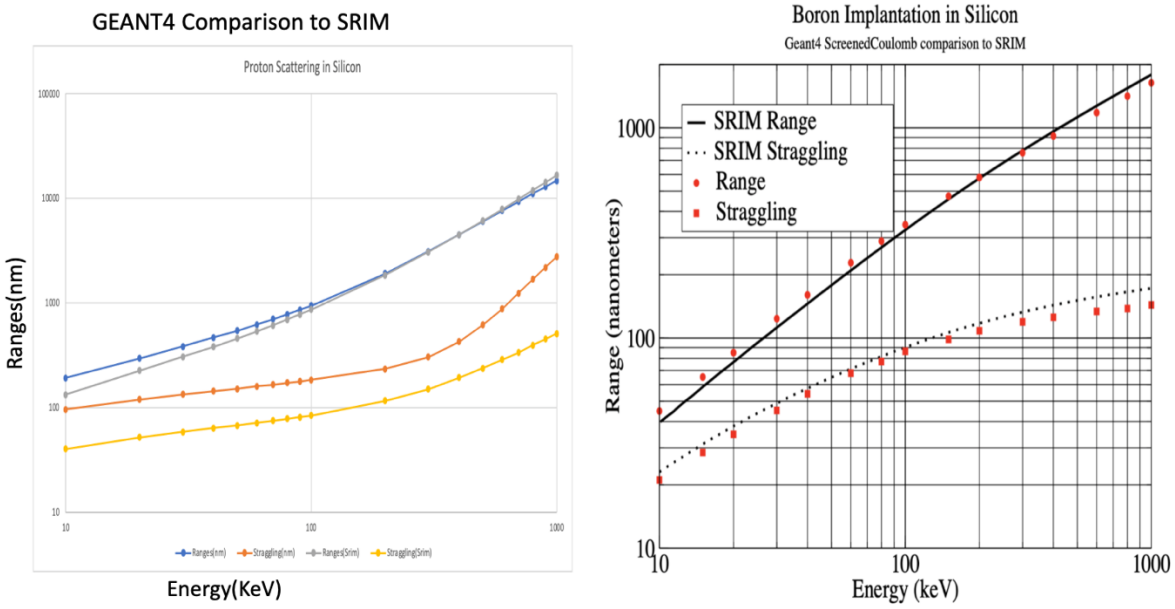

Figure 4. 10 Proton Scattering in Silicon Comparison to Boron Implantation in Silicon [7].

I used SRIM to construct a comparable proton scattering behaviour in silicon. I used several energies to compare GEANT4 with SRIM, and the outcome is depicted in the picture below.

Although one can observe the differences in behaviour, utilizing GEANT4's screened nuclear recoil model gives us greater confidence in these kinds of conclusions than we would otherwise have.

4.7 Effect of Thickness of Aluminum Layer on Energy Deposition with Total Energy

The Effect of Thickness of Aluminum Layer on Energy Deposition with Total Energy suggests an exploration into how the thickness of an aluminum layer influences the process of energy deposition, considering the total energy involved.

In experimental or computational studies related to material science or radiation physics, researchers often examine how the thickness of a material layer affects the way it interacts with incoming energy. In this case, the material of interest is aluminum. The "energy deposition" refers to the transfer of energy from an incoming source to the material, and the term "total energy" implies considering the entire energy content involved in the process.

Researchers are interested in understanding how varying the thickness of the aluminum layer impacts the amount of energy deposited within the material. This exploration could be relevant in various contexts, such as optimizing shielding materials, understanding radiation effects on materials of different thicknesses, or designing materials for specific applications where energy deposition plays a critical role. The study may involve experimental measurements, simulations, or a combination of both to quantify and analyze the observed effects.

The effect of aluminum layer thickness on overall energy was verified for GEANT4 and SRIM. SRIM loses more energy overall but still has some energy left in the end, whereas GEANT4 uses less energy overall.

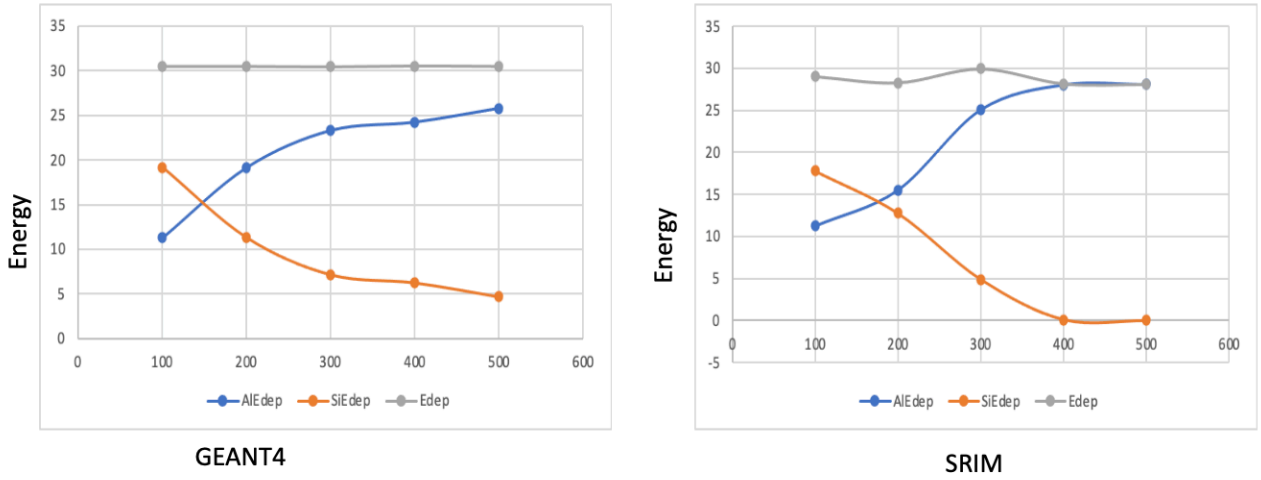

Figure 4. 11 Effect of Layers of Aluminum on Energy Deposition.

Chapter 5

Conclusion

5.1 BL3 Experiment

The experimental apparatus for the BL3 experiment was simulated, built, and optimized using a GEANT4-based simulation. A screened nuclear recoil model appropriate for low-energy proton-nucleus scattering was added to the physics list, which was used to simulate particle movement and interactions. This model was taken from one of GEANT4's examples. This will allow the considerably more open-ended GEANT4 architecture to incorporate a range of SRIM (Stopping and Range of Ions in Matter) software applications.

The energy deposition and backscattering/transmission of 35 keV protons on a silicon detector are investigated using the example in TestEm7/StandardNR, G4BL3/SNR, and the physics list in GEANT4. An analysis is being done to compare the results to SRIM and corroborate the energy accumulation in GEANT4's many processes and its impacts on the ratio of different components.

The beam method is the next-generation neutron lifetime experiment known as BL3 (Beam Lifetime 3). This follows a series of studies at ILL (France) and the NIST Neutron Research Center that have continued for over 30 years and produced the most accurate measurements of neutron lifetimes using beam technology.

A consistent and accurate experimental value is needed for the Neutron lifetime because it has significant consequences for particle physics, nuclear physics, and cosmology. Although trials with total uncertainty < 1 second have been documented, one cannot claim that the neutron lifetime is currently known with the required level of accuracy given the approximately 9-second difference. These new neutron lifetime experiments aim to clarify the reason(s) for the disparity and further our understanding of the neutron lifetime.

Today, a large scientific community from across the world uses the GEANT4 Toolkit in a variety of experimental fields. Both large-scale high-energy physics experiments and smaller-scale detector development programmes employ GEANT4 in production. It serves as the foundation for precise calculations in medical physics, nuclear medicine, and radiation protection. It is also used for accurate simulation in mission-critical space research and astrophysics applications.

To lower the uncertainties of the lifespan measurement, the BL3 experiment scales up the BL2, which is now placed at the NIST reactor. The diameter of the neutron beam will be increased from 10 mm to 35 mm, which will enhance the counting statistics. The BL3 team will address the technical issues specific to the beam approach to solve the neutron lifetime question. NSF has provided funding for the BL3 project to build a new magnet, a new proton trap, and new detection systems.

Bibliography

[1] Wietfeldt, F. E. “Measurements of the Neutron Lifetime.” Atoms, vol. 6, no. 4, 2018, pp. 70-, https://doi.org/10.3390/atoms6040070.

[2] “The Discovery of Fission.” Discovery of Fission - Michael Liu - PH204, Fall 2009, Stanford University, http://large.stanford.edu/courses/2009/ph204/liu1/.

[3] Space-based measurement of the neutron lifetime using data from neutron spectrometer on NASA’s Messenger mission Wilson, Jack T.; Lawrence, David J.; Peplowski, Patrick N. Eke, Vincent R.; Kegerreis, Jacob A. Physical review research, 2020, Vol.2 (2)

[4] Physicists make the most precise measurements ever of neutrons’ lifetime. Castelvecchi, Davide Nature (London), 2021, Vol.598 (7882), p.549-549

[5] Nico, J. S., et al. “Measurement of the Neutron Lifetime by Counting Trapped Protons in a Cold Neutron Beam.” Physical Review. C, Nuclear Physics, vol. 71, no. 5, 2005,

[6] Seestrom, Susan J., and Rhaimie Wahap. Next Generation Experiments to Measure the Neutron Lifetime: Santa Fe, New Mexico 9-10 November 2012. Edited by Susan J. Seestrom and Rhaimie Wahap, World Scientific, 2014.

[7] Mendenhall, Marcus H., and Robert A. Weller. “An Algorithm for Computing Screened Coulomb Scattering in GEANT4.” Nuclear Instruments & Methods in Physics Research. Section B, Beam Interactions with Materials and Atoms, vol. 227, no. 3, 2005, pp. 420–30, https://doi.org/10.1016/j.nimb.2004.08.014.

[8] Wietfeldt, F. E., et al. “A Path to a 0.1 s Neutron Lifetime Measurement Using the Beam Method.” Physics Procedia, vol. 51, 2014, pp. 54–58, https:/doi.org/10.1016/j.phpro. 2013.12.013.

[9] Hoogerheide, Shannon F., et al. “Progress on the BL2 Beam Measurement of the Neutron Lifetime.” EPJ Web of Conferences, vol. 219, 2019, p. 3002–, https:/doi.org/10.1051/epjconf/ 201921903002.

[10] Nico, J. S., et al. “Measurement of the Neutron Lifetime by Counting Trapped Protons in a Cold Neutron Beam.” Physical Review. C, Nuclear Physics, vol. 71, no. 5, 2005, https://doi.org/10.1103/PhysRevC.71.055502.

[11] “Toward to the Neutron Lifetime Puzzle, the 3rd Method Was Launched.” January 29, 2021 ICEPP THE UNIVERSITY OF TOKYO, https://www.icepp.s.u-tokyo.ac.jp/en/information/ 20210129. html.

[12] Hoogerheide, Shannon F. “Measuring the Neutron Lifetime with Record-Breaking Precision.” Physics (College Park, Md.), vol. 14, 2021, https://doi.org/10.1103/Physics.14.142.

[13] P. A. Zyla et al., “Review of particle physics”, Progress of Theoretical and Experimental Physics 2020, 083C01 (2020).

[14] “Screen Nuclear Recoil Method.” GEANT4.10: G4screenednuclearrecoil Class Reference, April 30, 2014 https://apc.u-paris.fr/~franco/g4doxy4.10/html/class_g4_screened_nuclear_ recoil. html.

[15] “Interactions of Ions with Matter.” James Ziegler (2010) - SRIM & TRIM, http://www.SRIM. org/.

[16] Fry, J., et al. “The Nab Experiment: A Precision Measurement of Unpolarized Neutron Beta Decay.” EPJ Web of Conferences, vol. 219, 2019, p. 4002–, https://doi.org/ 10.1051/ epjconf/201921904002.

[17] Broussard, Leah Jacklyn, et al. “Neutron Decay Correlations in the Nab Experiment” Journal of Physics. Conference Series, vol. 876, 2017, https://doi.org/10.1088/17426596/876/1/ 012005.

[18] Wietfeldt, F. E., et al. Comments on Systematic Effects in the NIST Beam Neutron Lifetime Experiment. 2022, https://doi.org/10.48550/arxiv.2209.15049.

[19] Schultz, Isaac. “Physicists Trap Ultracold Neutrons in a Bottle to See How Long They Live.” Gizmodo, Gizmodo, 19 Oct. 2021, https://gizmodo.com/physicists-trap-ultracold-neutrons-in-a-bottle-to-see-h-1847870808.

[20] Wolchover, Natalie, and substantive Quanta Magazine moderates’ comments to facilitate an informed. “Neutron Lifetime Puzzle Deepens, but No Dark Matter Seen.” Quanta Magazine, 31 Jan. 2019, https://www.quantamagazine.org/neutron-lifetime-puzzle-deepens-but-no-dark-matter-seen-20180213/.

[21] Gonzalez, F. M., et al. “Improved Neutron Lifetime Measurement with UCN τ.” Physical Review Letters, vol. 127, no. 16, 2021, pp. 162501–162501, https://doi.org/10.1103/ PhysRevLett.127.162501

[22] Wilson, Jack T., et al. “Measurement of the Free Neutron Lifetime Using the Neutron Spectrometer on NASA’s Lunar Prospector Mission.” Physical Review. C, vol. 104, no. 4, 2021, https://doi.org/10.1103/PhysRevC.104.045501.

[23] B. Hayes, Christopher. “Neutron Beta-Decay.” Neutron Beta Decay, Dec. 2012, aesop.phys.utk.edu/ph611/2012/projects/Hayes.pdf.